CHAPTER

21

The Circuitry

The circulatory, endocrine, and nervous systems constitute the principal coordinating and integrating systems of the body. The nervous system facilitates communications and the endocrine glands regulate certain body functions. The circulatory system serves to transport and distribute essential substances to the tissues and to remove byproducts of metabolism. The circulatory system also participates in homeostatic mechanisms such as regulation of body temperature, fluid maintenance, and adjustments of oxygen and nutrient supply in different physiological states.

The cardiovascular system that accomplishes these tasks is composed of a pump (the heart), a series of distributing and collecting tubes (the blood vessels), and an extensive system of thin vessels that permit rapid exchange between the tissues and the vascular channels (the capillaries). In this section, we discuss the function of these components of the vascular system and their control mechanisms (with their checks and balances). By altering the flow of blood to tissues, these control mechanisms are able to meet the changing requirements of different tissues in response to a variety of physiological and pathological conditions.

The function of the parts of the circulatory system is discussed in detail in subsequent chapters. This chapter provides a general, functional overview of the circulatory system.

■ *The Heart*

The heart consists of two pumps in series: one pump propels blood through the lungs for exchange of oxygen and carbon dioxide (the **pulmonary circulation**) and the other pump propels blood to all other tissues of the body (the **systemic circulation**). The flow of blood through the heart is one-way (unidirectional). Unidirectional flow through the heart is achieved by the appropriate arrangement of flap valves. Although the cardiac output is intermittent, continuous flow to the body tissues (periphery) occurs by distention of the aorta and its branches during ventricular contraction (**systole**) and by elastic recoil of the walls of the large arteries with forward propulsion of the blood during ventricular relaxation (**diastole**).

■ *Blood Vessels*

Blood moves rapidly through the aorta and its arterial branches. These branches narrow and their walls become thinner as they approach the periphery. They also change histologically. The aorta is a predominantly elastic structure, but the peripheral arteries become more muscular until at the arterioles the muscular layer predominates (Fig. 21-1).

In the large arteries, frictional resistance is relatively small and pressures are only slightly less than in the aorta. The small arteries, on the other hand, offer moderate resistance to blood flow. This resistance reaches a maximal level in the arterioles, which are sometimes referred to as the stopcocks of the vascular system. Hence, *the pressure drop is greatest across the terminal segment of the small arteries and the arterioles* (Fig. 21-2). Adjustment in the degree of contraction of the circular muscle of these small vessels permits regulation of tissue blood flow and aids in the control of arterial blood pressure.

In addition to the reduction in pressure along the arterioles, there is a change from a pulsatile to a steady blood flow (Fig. 21-3). *The **pulsatile arterial blood flow,** caused by the intermittent ejection of blood from the heart, is damped at the capillary level by a combination of two factors: distensibility of the large arteries and frictional resistance in the small arteries and arterioles.*

In a patient with hyperthyroidism (**Graves' disease**), the basal metabolism is elevated and is often associated with arteriolar vasodilation. This reduction in arteriolar resistance diminishes the damping effect on the pulsatile arterial pressure and is manifested as pulsatile flow in the capillaries, as observed in the finger nailbed of patients with this ailment.

Many capillaries arise from each arteriole. The total cross-sectional area of the capillary bed is very large, despite the fact that the cross-sectional area of each capillary is less than that of each arteriole. As a result, blood flow velocity becomes quite slow in the capillaries, analogous to the decrease in velocity of flow (Fig. 21-3) in the wide regions of a river. Because capillaries consist of short tubes with walls that are only one cell thick and because flow velocity is low, conditions in the capillaries are ideal for the exchange of diffusible substances between blood and tissue.

On its return to the heart from the capillaries, blood passes through venules and then through veins of increasing size. Pressure within these vessels progressively decreases until the blood reaches the right atrium (Fig. 21-2). Near the heart, the number of veins decreases, the thickness and composition of the vein walls change (Fig. 21-1), the total cross-sectional area of the venous chan-

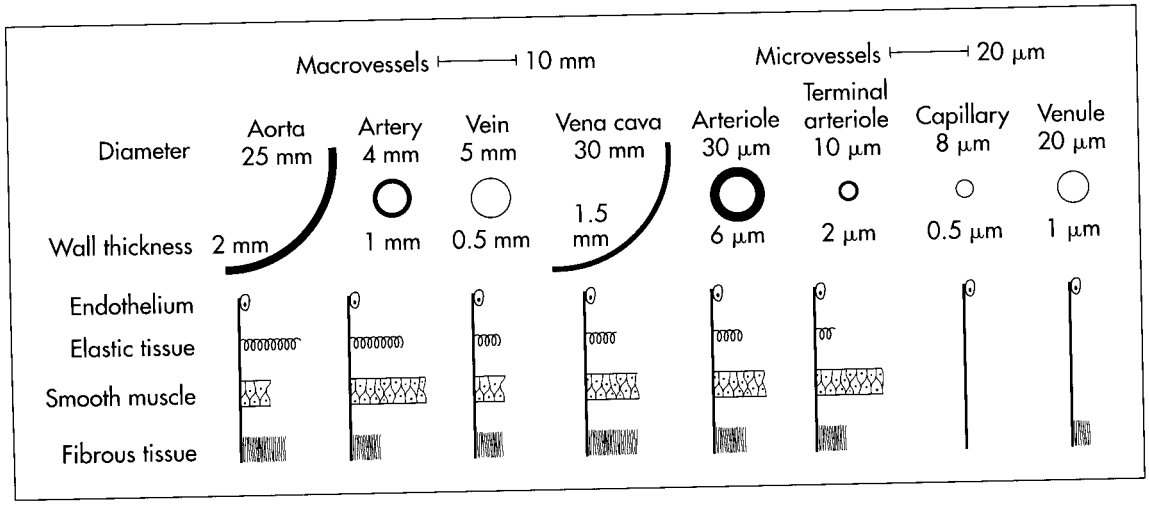

■ **Fig. 21-1** Internal diameter, wall thickness, and relative amounts of the principal components of the vessel walls of the various blood vessels that compose the circulatory system. Cross-sections of the vessels are not drawn to scale because of the huge range from aorta and venae cavae to capillary. (Redrawn from Burton AC: *Physiol Rev* 34:619, 1954.)

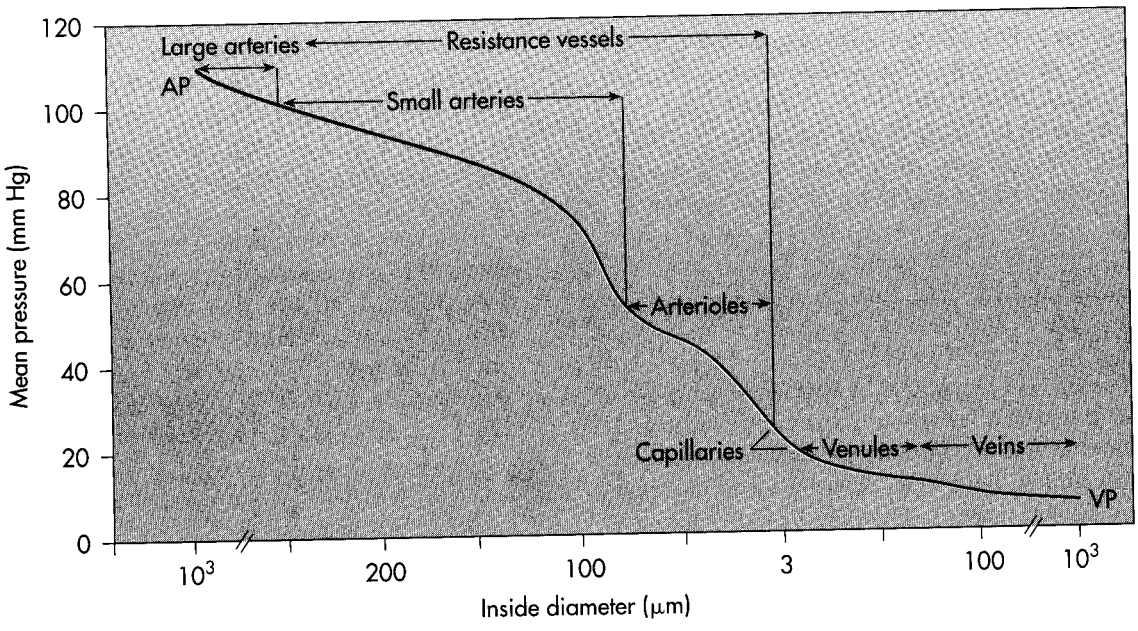

■ **Fig. 21-2** Pressure drop across the vascular system in the hamster cheek pouch. *AP,* Mean arterial pressure; *VP,* venous pressure. (Redrawn from David MJ et al: *Am J Physiol* 250:H291, 1986.)

nels diminishes, and the **velocity of blood flow** increases (Fig. 21-3). Note that the velocity of blood flow and the cross-sectional area at each level of the vasculature are essentially mirror images (Fig. 21-3).

Data from a 20-kg dog (Table 21-1) indicate that between the aorta and the capillaries the number of vessels increases about 3 billion-fold, and the total cross-sectional area increases about 500-fold. The volume of blood in the systemic vascular system is greatest in the veins and venules (67%). Only 5% of total blood volume exists in the capillaries, and 11% of total blood volume is found in the aorta, arteries, and arterioles. In contrast, blood volume in the pulmonary vascular bed is about equally divided among the arterial, capillary, and venous vessels. The cross-sectional area of the venae cavae is larger than that of the aorta. Therefore, the velocity of flow is slower in the venae cavae than that in the aorta (Fig. 21-3).

■ *The Cardiac Cycle*

Blood entering the right ventricle via the right atrium is pumped through the pulmonary arterial system at a mean pressure about one seventh that in the systemic arteries. The blood then passes through the lung capillaries, where carbon dioxide in the blood is released and oxygen is taken up. The oxygen-rich blood returns via the pulmonary veins to the left atrium, where it is pumped from the ventricle to the periphery, thus completing the cycle.

In the normal, intact circulation, the total volume of blood is constant, and an increase in the volume of blood in one area must be accompanied by a decrease in another. However, the distribution of the circulating blood to the different regions of the body is determined by the output of the left ventricle and by the contractile state of the resistance vessels (arterioles) of these regions.

■ **Table 21-1** Vascular dimensions in a 20-kg dog

Vessels	*No.*	*Total cross-sectional area (cm^2)*	*Total blood volume (%)*
Systemic			
Aorta	1	2.8	11
Arteries	40-110,000	40	
Arterioles	2.8×10^6	55	
Capillaries	2.7×10^9	1357	5
Venules	1×10^7	785	67
Veins	660,000-110	631	
Venae cavae	2	3.1	
Pulmonary			
Arteries and arterioles	$1\text{-}1.5 \times 10^6$	137	3
Capillaries	2.7×10^9	1357	4
Venules and veins	$1 \times 10^6\text{-}4$	210	5
Heart			
Atria	2		5
Ventricles	2		

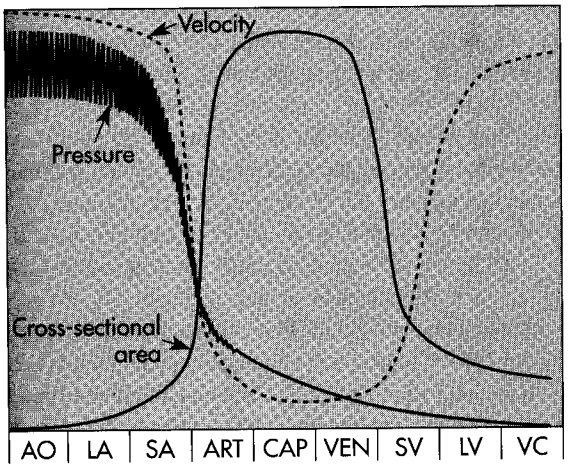

■ **Fig. 21-3** Phasic pressure, velocity of flow, and cross-sectional area of the systemic circulation. *The important features are the inverse relationship between velocity and cross- sectional area, the major pressure drop across the small arteries and arterioles, and the maximal cross-sectional area and minimal flow rate in the capillaries. AO,* Aorta; *LA,* large arteries; *SA,* small arteries; *ART,* arterioles; *CAP,* capillaries; *VEN,* venules; *SV,* small veins; *LV,* large veins; *VC,* venae cavae.

The circulatory system is composed of conduits arranged in series and in parallel (Fig. 21-4). This arrangement, which is discussed in subsequent chapters, has important implications in terms of resistance, flow, and pressure in the blood vessels.

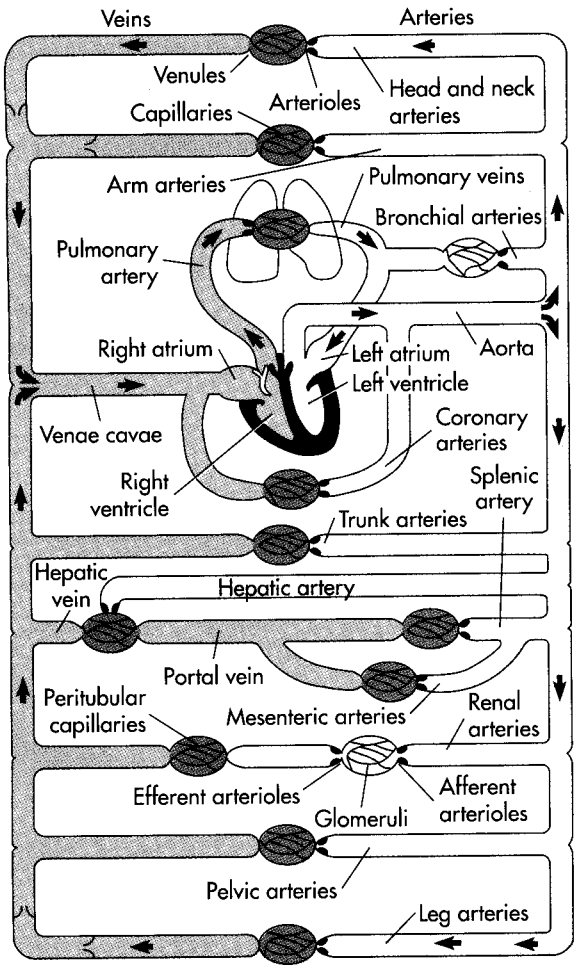

■ **Fig. 21-4** Schematic diagram of the parallel and series arrangement of the vessels composing the circulatory system. The capillary beds are represented by thin lines connecting the arteries *(on the right)* with the veins *(on the left)*. The crescent-shaped thickenings proximal to the capillary beds represent the arterioles (resistance vessels). (Redrawn from Green HD: In Glasser O, editor: *Medical physics,* vol 1, Chicago, 1944, Mosby–Year Book.)

■ *Summary*

1. The circulatory system consists of a pump (the heart), a series of distributing and collecting tubes (blood vessels), and an extensive system of thin vessels that permit rapid exchange of substances between the tissues and blood.

2. The greatest resistance to blood flow, and hence the greatest pressure drop, in the arterial system occurs at the level of the small arteries and the arterioles.

3. Pulsatile pressure is progressively damped by the elasticity of the arteriolar walls and the frictional resistance of the small arteries and arterioles, so that capillary blood flow is essentially nonpulsatile.

4. Velocity of blood flow is inversely related to the cross-sectional area at any point along the vascular system.

5. Most of the blood in the systemic vascular bed is located in the venous side of the circulation.

■ *Self-Study Problems*

1. What physical characteristics of arterioles enable them to maintain arterial blood pressure and to adjust the distribution of blood flow?

2. Why does most of the blood in the systemic circulation reside in the veins and venules?

3. Where in the systemic circulation is velocity of blood flow fastest and where is it slowest? Why?

4. Why is flow pulsatile in the systemic arterial system but nonpulsatile in the capillaries and venous systems?

CHAPTER

22

Electrical Activity of the Heart

Two centuries ago, Galvani and Volta demonstrated that electrical phenomena were involved in the spontaneous contractions of the heart. In 1855, Kölliker and Müller found that when they placed the nerve of an innervated skeletal muscle preparation in contact with the surface of a beating frog's heart, the skeletal muscle twitched with each cardiac contraction. The researchers concluded that the spontaneous excitation of the heart had generated sufficient electrical activity to excite the motor nerve fibers and stimulate the skeletal muscle.

The electrical events that normally take place in the heart initiate cardiac contraction. Disorders in electrical activity can induce serious and sometimes lethal disturbances in the cardiac rhythm.

■ *Transmembrane Potentials*

To investigate the electrical behavior of single cardiac cells, researchers insert a microelectrode into the interior of the cell. The microelectrode is attached to a galvanometer, a device that measures the strength of an electrical current. The potential changes recorded from a typical ventricular muscle fiber are illustrated in Fig. 22-1, *A*. When two electrodes are placed in an electrolyte solution near a strip of quiescent cardiac muscle, no potential difference (point *a*) is measurable between the two electrodes. At point *b*, when one of the electrodes is inserted into the interior of a cardiac muscle fiber (Fig. 22-1), the galvanometer immediately records a potential difference (V_m) across the cell membrane. The potential of the interior of the cell is about 90 mV lower than that of the surrounding medium. This electronegativity of the interior of the resting cell with respect to the exterior is also characteristic of skeletal and smooth muscle, nerves, and most cells within the body (see also Chapter 2).

At point *c*, the ventricular cell is excited by an electronic stimulator, and the cell membrane rapidly depolarizes. During depolarization, the potential difference is actually reversed, such that the potential of the interior of the cell exceeds that of the exterior by about 20 mV. The rapid **upstroke** of the action potential is designated **phase 0.** The upstroke is followed immediately by a brief period of partial, **early repolarization (phase 1),** and then by a **plateau (phase 2)** that persists for about 0.1 to 0.2 second. The membrane then repolarizes **(phase 3)** until the resting state of polarization **(phase 4)** is again attained (at point *e*). **Final repolarization** (phase 3) develops more slowly than does depolarization (phase 0).

The relationships between the electrical events in the cardiac muscle and actual contraction of the cardiac muscle are shown in Fig. 22-2. Rapid depolarization (phase 0) occurs before force develops, and completion of repolarization coincides approximately with peak force. The relaxation of the muscle takes place mainly during phase 4 of the action potential. The duration of contraction parallels the duration of the action potential.

■ *Principal Types of Cardiac Action Potentials*

Two main types of action potentials take place in the heart and are shown in Fig. 22-1. One type, the **fast response,** occurs in normal atrial and ventricular myocytes and the specialized conducting fibers (**Purkinje** fibers of the heart). The other type of action potential, the **slow response,** occurs in the **sinoatrial (SA) node,** the natural pacemaker region of the heart, and in the **atrioventricular (AV) node,** the specialized tissue that conducts the cardiac impulse from atria to ventricles.

Fast responses may change to slow responses under certain pathological conditions. For example, in coronary artery disease, a region of cardiac muscle is deprived of its normal blood supply. As a result, the K^+ concentration in the interstitial fluid that surrounds the affected muscle cells rises because K^+ is lost from the inadequately perfused (or **ischemic**) cells. The action potentials in some of these cells may then be converted from fast to slow responses. An experimental conversion from a fast to a slow response is illustrated in Fig. 22-14.

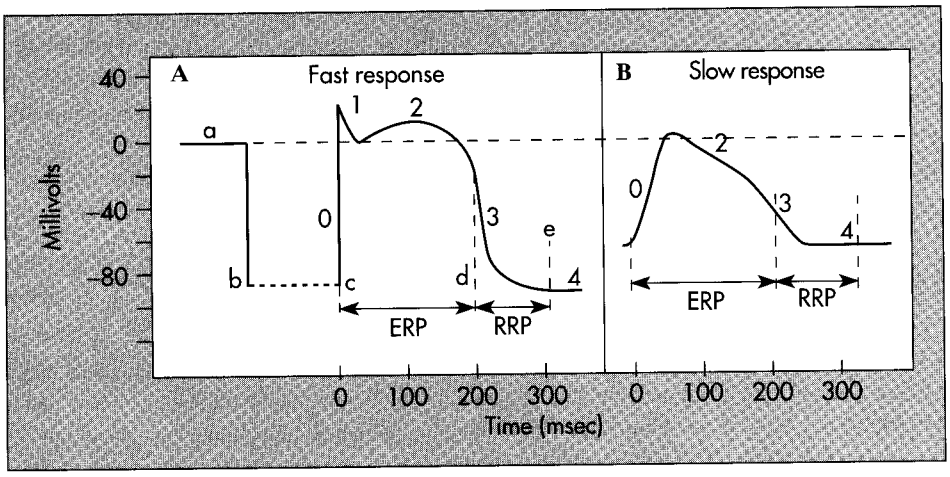

■ **Fig. 22-1** Changes in transmembrane potential recorded from a fast-response and a slow-response cardiac fiber in isolated cardiac tissue immersed in an electrolyte solution. **A,** At time *a* the microelectrode was in the solution surrounding the cardiac fiber. At time *b* the microelectrode entered the fiber. At time *c* an action potential was initiated in the impaled fiber. Time *c* to *d* represents the effective refractory period (*ERP*), and time *d* to *e* represents the relative refractory period (*RRP*). **B,** An action potential recorded from a slow-response cardiac fiber. Note that, compared with the fast-response fiber, the resting potential of the slow fiber is less negative, the upstroke (phase *0*) of the action potential is less steep, the amplitude of the action potential is smaller, phase *1* is absent, and the relative refractory period (*RRP*) extends well into phase *4* after the fiber has fully repolarized.

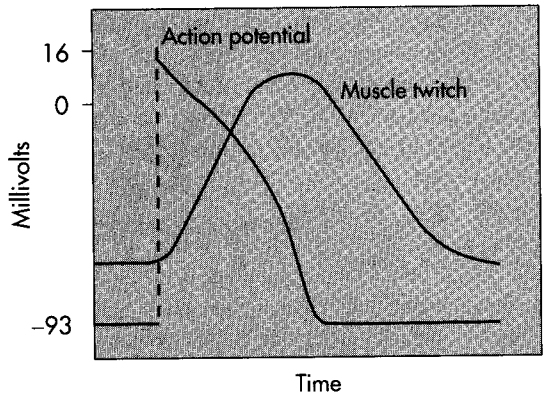

■ **Fig. 22-2** Time relationships between the developed force and the changes in transmembrane potential in a thin strip of ventricular muscle. (Redrawn from Kavaler F, Fisher VJ, Stuckey JH: *Bull N Y Acad Med* 41:592, 1965.)

As shown in Fig. 22-1, not only is the resting membrane potential (phase 4) of the fast response considerably more negative than that of the slow response, but the slope of the upstroke (phase 0), the amplitude of the action potential, and the extent of the overshoot of the fast response are greater than in the slow response. The amplitude of the action potential and the steepness of the upstroke are important determinants of how fast the action potential is propagated. In slow-response cardiac tissue, the action potential is propagated more slowly than in fast-response cardiac tissue. In addition, the conduction is more likely to be blocked in slow-response cardiac tissue than in fast-response tissue. Slow conduction and a tendency toward conduction block increase the likelihood of some rhythm disturbances.

■ *Ionic Basis of the Resting Potential*

The various phases of the cardiac action potential are associated with changes in the permeability of the cell membrane, mainly to sodium, potassium, and calcium ions. Changes in cell membrane permeability alter the movement of these ions across the membrane. The permeability of the membrane to a given ion, its transmembrane concentration difference, and the transmembrane electrical potential difference define the net quantity of the ion that will diffuse across the membrane. Changes in permeability are accomplished by the opening and closing of ion channels that are specific for the individual ions.

As with all other cells in the body (see also Chapter 2), the concentration of potassium ions inside a cardiac muscle cell ($[K^+]_i$) is far greater than the concentration outside the cell ($[K^+]_o$) (Fig. 22-3). The reverse concentration gradient exists for sodium and calcium ions. Estimates of the extracellular and intracellular concentrations of Na^+, K^+, and Ca^{++} and the equilibrium potentials (this term is defined later in this chapter) for these ions are compiled in Table 22-1.

The resting cell membrane is relatively permeable to K^+ but much less so to Na^+ and Ca^{++}. Hence, K^+ tends to diffuse from the inside to the outside of the cell in the direction of the K^+ concentration gradient, as shown on the right side of the cell in Fig. 22-3.

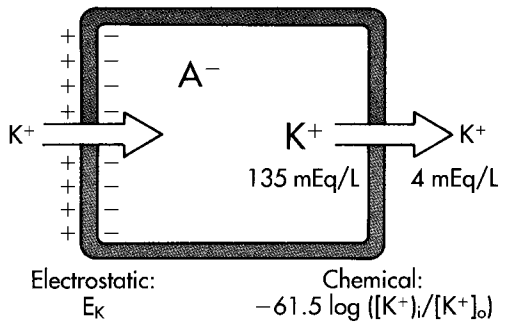

■ **Fig. 22-3** The balance of chemical and electrostatic forces acting on a resting cardiac cell membrane. The estimations are based on a 34:1 ratio of the intracellular to extracellular K^+ concentrations and the existence of a nondiffusible anion (A^-) inside, but not outside, the cell.

■ **Table 22-1** Intracellular and extracellular ion concentrations and equilibrium potentials in cardiac muscle cells

Ion	*Extracellular concentrations (mM)*	*Intracellular concentrations (mM)**	*Equilibrium potential (mV)*
Na^+	145	10	70
K^+	4	135	−94
Ca^{++}	2	10^{-4}	132

Modified from Ten Eick RE, Baumgarten CM, Singer DH: *Prog Cardiovasc Dis* 24:157, 1981.
*The intracellular concentrations are estimates of the free concentrations in the cytoplasm

Any flux of K^+ that occurs during phase 4 takes place mainly through specific **K^+ channels.** Several types of K^+ channels exist in cardiac cell membranes. Some of these channels are regulated (i.e., they open and close) according to the transmembrane potential, whereas others are regulated by a chemical signal (e.g., the extracellular acetylcholine concentration). One of the specific K^+ channels through which K^+ passes during phase 4 is a voltage-regulated channel that conducts the **inwardly rectifying K^+ current.** This current is symbolized i_{K1}, and is discussed in more detail later (Fig. 22-8). For now, it is only necessary to know how this current is established. Many of the anions (labeled A^-), such as the proteins, inside the cell, are not free to diffuse out with the K^+ (Fig. 22-3). Therefore, the K^+ diffuses out of the cell and leaves the impermeant A^- behind. The deficiency of cations then causes the interior of the cell to become electronegative (see also Chapter 2). As a result, the positively charged K^+ ions are attracted to the interior of the cell by the negative potential that exists there, as shown on the left side of the cell in Fig. 22-3.

Therefore, two opposing forces are involved in the movement of K^+ across the cell membrane. A chemical force, based on the concentration gradient, results in net outward diffusion of K^+. The counterforce is based on electrostatic differences between the interior and exterior of the cell. If the system came into equilibrium, the chemical and the electrostatic forces would be equal. As explained in Chapter 2, this equilibrium is expressed by the **Nernst equation** for potassium:

$$E_K = 61.5 \log([K^+]_i/[K^+]_o)$$

The right-hand term represents the chemical potential difference, and the left-hand term, E_K, represents the electrostatic potential difference that would exist across the cell membrane if K^+ were the only diffusible ion. E_K is called the **potassium equilibrium potential.**

When the measured concentrations of $[K^+]_i$ and $[K^+]_o$ for mammalian myocardial cells are substituted into the Nernst equation, the calculated value of E_K equals about −95 mV (Table 22-1). This value is close to, but slightly more negative than, the resting potential actually measured in myocardial cells. Therefore, the potential that tends to drive K^+ out of the resting cell is small. The actual resting potential is slightly less negative than the predicted potential because the cell membrane is slightly permeable to other ions, notably to Na^+. The balance of the forces acting on Na^+ is opposite to the balance of forces acting on K^+ in resting cardiac cells. The intracellular Na^+ concentration, $[Na^+]_i$, is much lower than the extracellular concentration, $[Na^+]_o$. The sodium equilibrium potential, E_{Na}, expressed by the Nernst equation, is about 70 mV (Table 22-1).

At equilibrium, therefore, an electrostatic force of about 70 mV, oriented with the inside of the cell more positive than the outside, is necessary to counterbalance the chemical potential for Na^+. However, as we have seen, the actual resting membrane potential of myocytes is about −90 mV. Hence, both chemical and electrostatic forces act to pull extracellular Na^+ into the cell. The influx of Na^+ through the membrane is small, however, because the membrane of the resting cell is not very permeable to Na^+. Nevertheless, this small inward current of Na^+ is sufficient to cause the potential (V_m) on the inside of the resting cell membrane to be slightly less negative than the value (E_K) predicted by the Nernst equation for K^+ (Fig. 22-4).

The dependence of V_m on the conductances and on the intracellular and extracellular concentrations of K^+, Na^+, and other ions is described by the **chord conductance equation,** as explained in Chapter 2. This equation reveals that relative—not absolute—membrane conductances to Na^+ and K^+ determine the resting potential. In the resting cardiac cell, the conductance (g_K) to K^+ is about 100 times greater than the conductance (g_{Na}) to Na^+. Therefore, the chord conductance equation reduces essentially to the Nernst equation for K^+. Because g_{Na} is so small in the resting cell, changes in external Na^+ concentration do not significantly affect V_m (Fig. 22-5).

When the ratio $[K^+]_i/[K^+]_o$ is decreased experimentally by raising $[K^+]_o$ in a suspension of myocytes, the measured value of V_m approximates the value of E_K predicted by the Nernst equation (Fig. 22-4). For extracellular K^+

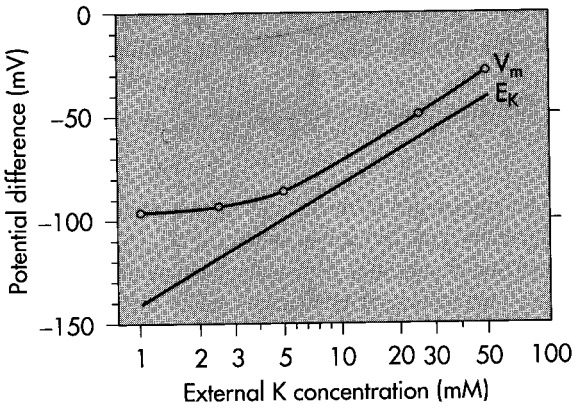

■ **Fig. 22-4** Transmembrane potential (V_m) of a cardiac muscle fiber varies inversely with the potassium concentration of the external medium. The straight line (E_K) represents the change in transmembrane potential predicted by the Nernst equation for potassium. (Redrawn from Page E: *Circulation* 26:582, 1962, with permission of the American Heart Association.)

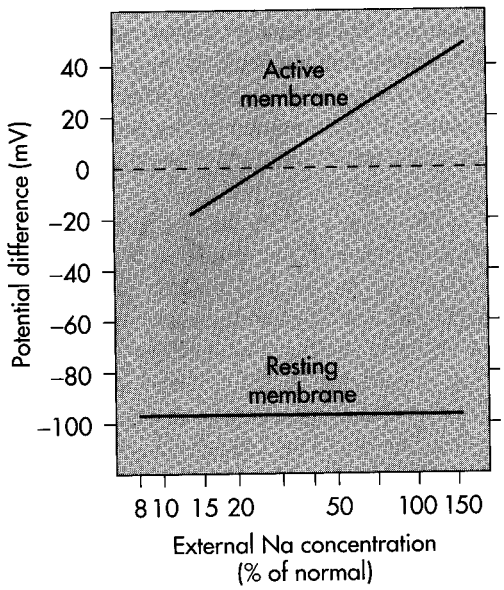

■ **Fig. 22-5** Concentration of sodium in the external medium is a critical determinant of the amplitude of the action potential in cardiac muscle (*upper line*) but it has very little influence on the resting membrane potential (*lower line*). (Redrawn from Weidmann S: *Elektrophysiologie der Herzmuskelfaser,* Bern, 1956, Verlag Hans Huber.)

concentrations greater than about 5 mM, the measured values correspond closely with the predicted values. The measured levels are only slightly less than those predicted by the Nernst equation because g_K is so much greater than g_{Na}. However, for values of $[K^+]_o$ below about 5 mM, g_K decreases as $[K^+]_o$ is diminished. As g_K decreases, the effect of g_{Na} on the transmembrane potential becomes relatively more significant, as predicted by the chord conductance equation. This change in g_K accounts for the greater deviation of the measured V_m from the value predicted by the Nernst equation for K^+ at low levels of $[K^+]_o$.

■ *Ionic Basis of the Fast Response*

■ *Phase 0: Genesis of the Upstroke*

Any stimulus that abruptly changes the resting membrane potential to a critical value (called the **threshold**) results in an action potential. The characteristics of fast response action potentials are shown in Fig. 22-1, *A*. The rapid depolarization (phase 0) is related almost exclusively to the influx of Na^+ into the myocyte due to a sudden increase in g_{Na}. The **amplitude** of the action potential (the potential change during phase 0) varies linearly with the logarithm of $[Na^+]_o$, as shown in Fig. 22-5. When $[Na^+]_o$ is reduced from its normal value of about 140 mM to about 20 mM, the cell is no longer excitable.

The physical and chemical forces responsible for these transmembrane movements of Na^+ are diagrammed in Fig. 22-6. When the resting membrane potential, V_m, is suddenly changed to the threshold level of about −65 mV, the properties of the cell membrane change dramatically. Na^+ enters the myocyte through specific **fast Na^+ channels** that exist in the membrane (see also Chapter 3). These channels can be blocked by the puffer fish toxin, **tetrodotoxin.** Also, many of the drugs used to treat certain cardiac rhythm disturbances **(cardiac arrhythmias)** act by blocking these fast Na^+ channels.

The manner in which Na^+ moves through these fast channels suggests that the flux is controlled by two types of **gates** in each channel. One of these, the **m gate,** tends to open the channel as V_m becomes less negative. This is therefore called an **activation gate.** The other gate, the **h gate,** tends to close the channel as V_m becomes less negative and hence is called an **inactivation gate.** The "m" and "h" designations were originally employed by Hodgkin and Huxley in their mathematical model of impulse conduction in nerve fibers.

As we have seen, the V_m of a resting cell is about −90 mV. The m gates are closed and the h gates are wide open, as shown in Fig. 22-6, *A*. Because the concentration of Na^+ outside the cell is greater than the Na^+ concentration inside the cell, the interior of the cell is electrically negative with respect to the exterior. Hence, both chemical and electrostatic forces are oriented to draw Na^+ into the cell.

The electrostatic force in Fig. 22-6, *A*, is a potential difference of 90 mV, and it is represented by the white arrow. The chemical force, based on the difference in Na^+ concentration between the outside and inside of the cell, is represented by the black arrow. For a Na^+ concentration difference of about 130 mM, a potential difference of 60 mV (with the inside more positive than outside) is necessary to counterbalance the chemical, or diffusional, force, according to the Nernst equation for Na^+. Therefore, the net chemical force that favors the inward movement of Na^+ in Fig. 22-6 (*black arrows*) is equivalent to a potential difference of 60 mV. In the resting cell, the total electrochemical force that favors the inward movement of Na^+ is 150 mV (*A*). The m gates are closed,

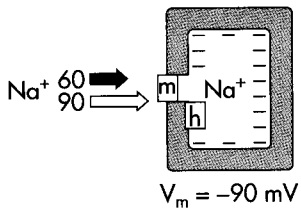

A, During phase 4, the chemical (60 mV) and electrostatic (90 mV) forces favor influx of Na^+ from the extracellular space. Influx is negligible, however, because the activation *(m)* gates are closed.

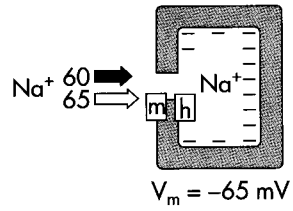

B, If V_m is brought to about −65 V, the *m* gates begin to swing open, and Na^+ begins to enter the cell. This reduces the negative charge inside the cell, and thereby opens still more Na^+ channels, which accelerates the influx of Na^+. The change in V_m also initiates the closure of inactivation *(h)* gates, which operate more slowly than the *m* gates.

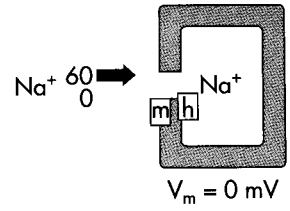

C, The rapid influx of Na^+ sharply decreases the negativity of V_m. As V_m approaches 0, the electrostatic force attracting Na^+ into the cell is neutralized. Na^+ continues to enter the cell, however, because of the substantial concentration gradient, and V_m begins to become positive.

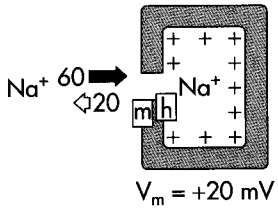

D, When V_m is positive by about 20 mV, Na^+ continues to enter the cell, because the diffusional forces (60 mV) exceed the opposing electrostatic forces (20 mV). The influx of Na^+ is slow, however, because the net driving force is small, and many of the inactivation gates have already closed.

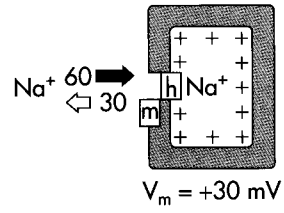

E, When V_m reaches about 30 mV, the *h* gates have now all closed, and Na^+ influx ceases. The *h* gates remain closed until the first half of repolarization, and thus the cell is absolutely refractory during this entire period. During the second half of repolarization, the *m* and *h* gates approach the state represented by panel *A*, and thus the cell is relatively refractory.

■ **Fig. 22-6** The gating of a sodium channel in a cardiac cell membrane during phase 4 **(A)** and during various stages of the action potential upstroke **(B** to **E).** The positions of the *m* and *h* gates in the fast Na^+ channels are shown at the various levels of V_m. The electrostatic forces are represented by the white arrows and the chemical (diffusional) forces by the black arrows.

however, and the conductance of the resting cell membrane to Na^+ is low. Therefore, in resting state, virtually no Na^+ moves into the cell.

Any stimulus that makes V_m less negative tends to open the m gates, and thereby tends to activate the fast Na^+ channels. The precise potential required to open the m gates and thus activate the Na^+ channels varies somewhat from one channel to another in the cell membrane. As V_m becomes progressively less negative, more and more m gates swing open, and the influx of Na^+ accelerates (Fig. 22-6, *B*). The entry of Na^+ into the interior of the cell neutralizes some of the negative charges within the cell, and thereby makes V_m still less negative. The consequent change in V_m then opens more m gates and augments the inward Na^+ current. This process is called **regenerative.** As V_m approaches about −65 mV, the remaining m gates rapidly swing open in the fast Na^+ channels until virtually all the m gates are open (Fig. 22-6, *B*).

The rapid opening of the m gates in the fast Na^+ channels is responsible for the large and abrupt increase in Na^+ conductance (g_{Na}) that occurs in phase 0 (the upstroke) of the action potential (Fig. 22-7). The rapid influx of Na^+ accounts for the steepness of the upstroke of the action potential. The maximal rate of change of V_m varies from 100 to 200 V/sec in myocardial cells and from 500 to 1000 V/sec in Purkinje fibers. Although Na^+ that enters the cell during one action potential alters V_m by more than 100 mV, the actual quantity of Na^+ that enters the cell is so small that the resultant change in the intracellular Na^+ concentration cannot be measured. Hence, the chemical force remains virtually constant, and only the electrostatic force changes throughout the action potential. In Fig. 22-6, note that the lengths of the black arrows remain constant (denoting a chemical force of 60 mV), while the white arrows change in magnitude and direction.

As Na^+ rushes into the cardiac cell during phase 0, the negative charges inside the cell are neutralized, and V_m becomes progressively less negative. When V_m falls to zero (Fig. 22-6, *C*), an electrostatic force no longer exists to pull Na^+ into the cell. As long as the fast Na^+ channels are open, however, Na^+ continues to enter the cell because of the large concentration gradient. This continuation of

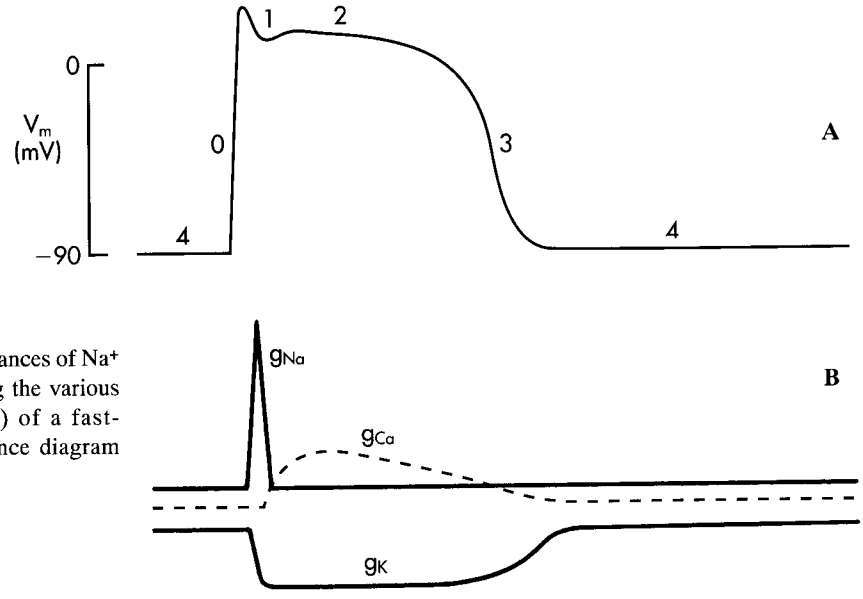

■ **Fig. 22-7** Changes in the conductances of Na^+ (g_{Na}), Ca^{++} (g_{Ca}), and K^+ (g_K) during the various phases of the action potential (**A**) of a fast-response cardiac cell. The conductance diagram (**B**) shows directional changes only.

the inward Na^+ current causes the inside of the cell to become positively charged (Fig. 22-6, *D*). This reversal of the membrane polarity is the so-called **overshoot** of the cardiac action potential. Such a reversal of the electrostatic gradient would, of course, tend to repel the entry of additional Na^+ (Fig. 22-6, *D*). However, as long as the inwardly directed chemical forces exceed the outwardly directed electrostatic forces, the net flux of Na^+ is directed inward, although the rate at which Na^+ enters the cell diminishes.

The inward Na^+ current finally stops when the h (inactivation) gates close (Fig. 22-6, *E*). Like the activity of the m gates, the activity of the h gates is governed by the value of V_m. However, the m gates open very rapidly (in about 0.1 msec), whereas the closure the h gates requires a few milliseconds. Phase 0 is finally terminated when all of the h gates have closed, thereby inactivating the fast Na^+ channels. The closure of the h gates so soon after the opening of the m gates accounts for the quick return of g_{Na} from its maximum to its resting value (Fig. 22-7).

The h gates then remain closed until the cell has partially repolarized during phase 3 (at about time *d* in Fig. 22-1, *A*). From time *c* to time *d* the cell is in its **effective refractory period** and will not respond to further excitation. This mechanism prevents a sustained, tetanic contraction of cardiac muscle. *Tetanic contraction of the ventricular myocytes would retard ventricular relaxation and therefore interfere with the normal intermittent pumping action of the heart.*

About midway through phase 3 (time *d* in Fig. 22-1, *A*), the m and h gates in some of the fast Na^+ channels have resumed the states shown in Fig. 22-6, *A*. Such channels are said to have **recovered from inactivation.** The cell can begin to respond (but weakly at first) to further excitation (Fig. 22-15). Throughout the remainder of phase 3 the cell completes its recovery from inactivation. By time *e* in Fig. 22-1, *A*, the h gates have reopened and the m gates have reclosed in all the fast Na^+ channels; that is, they have resumed the status depicted in Fig. 22-6, *A*.

■ *Phase 1: Genesis of Early Repolarization*

In many cardiac cells that have a prominent plateau, phase 1 constitutes an early, brief period of limited repolarization. In Fig. 22-1, this brief repolarization is represented by a notch between the end of the upstroke and the beginning of the plateau. Repolarization occurs briefly owing to the activation of a **transient outward current** ($\mathbf{i_{to}}$), carried mainly by K^+. Activation of K^+ channels during phase 1 causes a brief efflux of K^+ from the cell, because the interior of the cell is positively charged and because the internal K^+ concentration greatly exceeds the external K^+ concentration (Fig. 22-8). As a result of this transient efflux of positively charged ions, the cell is briefly and partially repolarized (phase 1).

The phase 1 notch is prominent in ventricular Purkinje fibers (Fig. 22-13) and in myocytes located in the epicardial and midmyocardial regions of the ventricular wall (Fig. 22-9). However, the notch is negligible in myocytes from the endocardial region (Fig. 22-9). The cycle length of depolarization also appears to affect phase 1. When the basic cycle length at which the epicardial and midmyocardial fibers are depolarized is increased from 300 to 8000 msec, the phase 1 notch becomes more pronounced and the action potential duration is increased substantially. The same increase in basic cycle length in endocardial fibers has no effect on phase 1 and only a small effect on the action potential duration (Fig. 22-9). In the presence of 4-aminopyridine, which blocks the K^+ channels that carry i_{to}, the phase 1 notch becomes much less prominent in the action potentials recorded from the epicardial and midmyocardial regions of the ventricles.

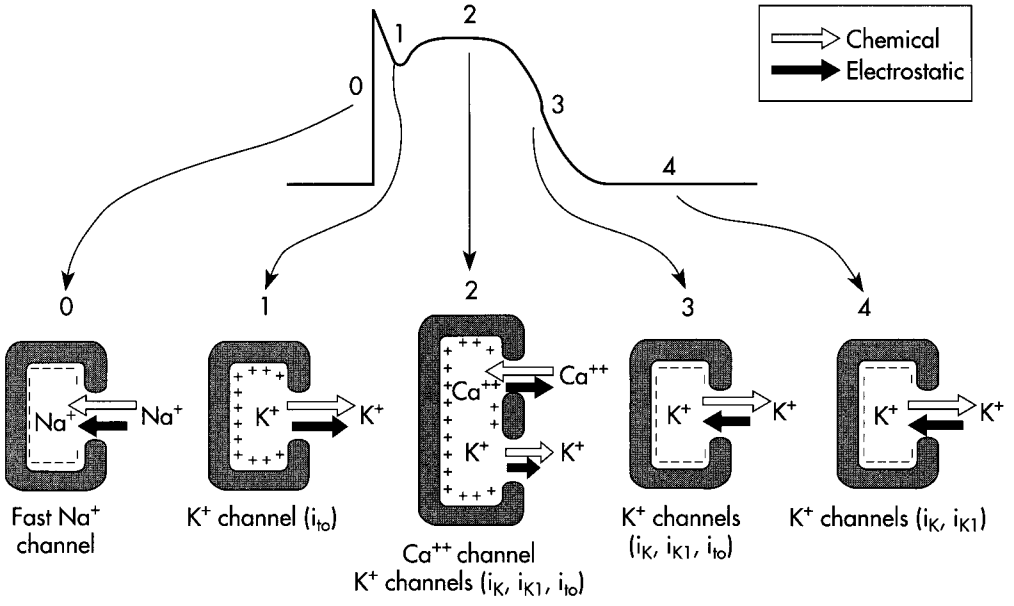

■ **Fig. 22-8** The principal ionic currents and channels that generate the various phases of the action potential in a cardiac cell. Phase 0: The chemical and electrostatic forces both favor the entry of Na^+ into the cell through fast Na^+ channels to generate the upstroke. Phase 1: The chemical and electrostatic forces both favor the efflux of K^+ through i_{to} channels to generate early, partial repolarization. Phase 2: During the plateau, the net influx of Ca^{++} through Ca^{++} channels is balanced by the efflux of K^+ through i_K, i_{K1}, and i_{to} channels. Phase 3: The chemical forces that favor the efflux of K^+ through i_K, i_{K1}, and i_{to} channels predominate over the electrostatic forces that favor the influx of K^+ through these same channels. Phase 4: The chemical forces that favor the efflux of K^+ through i_K and i_{K1} channels exceed very slightly the electrostatic forces that favor the influx of K^+ through these same channels.

■ *Phase 2: Genesis of the Plateau*

During the plateau of the action potential, Ca^{++} enters the myocardial cells through **calcium channels,** which activate and inactivate much more slowly than do the fast Na^+ channels. During the flat portion of phase 2 (Fig. 22-8), this influx of positive charge carried by Ca^{++} is counterbalanced by the efflux of positive charge carried by K^+. K^+ exits through channels that conduct mainly the i_{to}, i_K, and i_{K1} currents. The i_{to} current is responsible for phase 1, as described previously, but it is not completely inactivated until after phase 2 has expired. The i_K and i_{K1} currents are described later in this chapter.

Ca^{++} conductance during the plateau. The Ca^{++} channels are voltage-regulated channels that are activated as V_m becomes progressively less negative during the upstroke of the action potential. Various types of Ca^{++} channels have been identified in cardiac tissues (see Chapter 3), but this discussion concentrates on the predominant channel, the so-called L-type Ca^{++} channel. Some of the important characteristics of this channel are illustrated in Fig. 22-10, which also shows the Ca^{++} currents generated by voltage-clamping an isolated atrial myocyte. Note that when V_m is suddenly increased to +30 mV from a holding potential of −30 mV, an inward Ca^{++} current is activated. Note also that after the inward current reaches its maximal value (in the downward direction), it returns to zero only very gradually (i.e., the channel inactivates very slowly). Thus, because the current that passes through these channels is long-lasting, the channels are designated "L-type."

Opening of the Ca^{++} channels is reflected by an increase in Ca^{++} conductance (g_{Ca}) immediately after the upstroke of the action potential (Fig. 22-7). At the beginning of the action potential, the intracellular Ca^{++} concentration is much less than the extracellular concentration (Table 22-1). Consequently, the increase in g_{Ca} promotes an influx of Ca^{++} into the cell throughout the plateau. *This influx of Ca during the plateau is involved in excitation-contraction coupling,* as described in Chapters 17 and 23.

Various factors, such as neurotransmitters and drugs, may substantially influence g_{Ca}. The adrenergic neurotransmitter **norepinephrine,** the β-adrenergic receptor agonist **isoproterenol,** and various other **catecholamines** may enhance Ca^{++} conductance, whereas the parasympathetic neurotransmitter **acetylcholine** may decrease Ca^{++} conductance. The enhancement of Ca^{++} conductance by catecholamines is probably the principal mechanism by which they enhance cardiac muscle contractility.

To enhance Ca^{++} conductance, catecholamines first interact with **β-adrenergic receptors** in the cardiac cell

membrane. This interaction stimulates the membrane-bound enzyme **adenylyl cyclase,** which raises the intracellular concentration of **cyclic adenosine monophosphate (cAMP)** (see also Chapter 5). The rise in the level of cAMP enhances the activation of the L-type Ca^{++} channels in the cell membrane (Fig. 22-10) and thus augments the influx of Ca^{++} into the cells from the interstitial fluid. Conversely, acetylcholine interacts with **muscarinic receptors** in the cell membrane to inhibit adenylyl cyclase. In this way, acetylcholine antagonizes the activation of Ca^{++} channels, and thereby diminishes g_{Ca}.

The **Ca^{++} channel antagonists** are substances that block Ca^{++} channels. Examples include the drugs **verapamil** and **diltiazem.** These drugs decrease g_{Ca}, thereby impeding the influx of Ca^{++} into myocardial cells. The Ca^{++} channel antagonists decrease the duration of the action potential plateau and diminish the strength of the cardiac contraction (Fig. 22-11). Paradoxically, although Ca^{++} channel antagonists have a depressant effect on the contractile strength of the heart, these agents are used widely in the treatment of **congestive heart failure,** a common clinical condition in which the contractile performance of the heart is already compromised. As a result, the heart is unable to generate enough blood flow to meet the needs of the tissues. The Ca^{++} channel antagonists weaken the cardiac contraction and depress the contraction of the vascular smooth muscle, thereby inducing generalized vasodilation. This diminished vascular resistance reduces the counterforce **(afterload)** that opposes the propulsion of blood from the ventricles into the arterial system, as explained in Chapters 25 and 26. Hence, vasodilator drugs, such as the Ca^{++} channel antagonists, are often referred to as **afterload-reducing drugs.** This ability to diminish the counterforce leads to a more adequate cardiac output, despite the direct cardiac depressant effect of these drugs.

K^+ conductance during the plateau. During the plateau of the action potential, the concentration gradient for K^+ across the cell membrane is virtually the same as it is during phase 4, but V_m is positive. Therefore, both the chemical and the electrostatic forces favor the efflux of K^+ from the cell (Fig. 22-8). If g_K were the same dur-

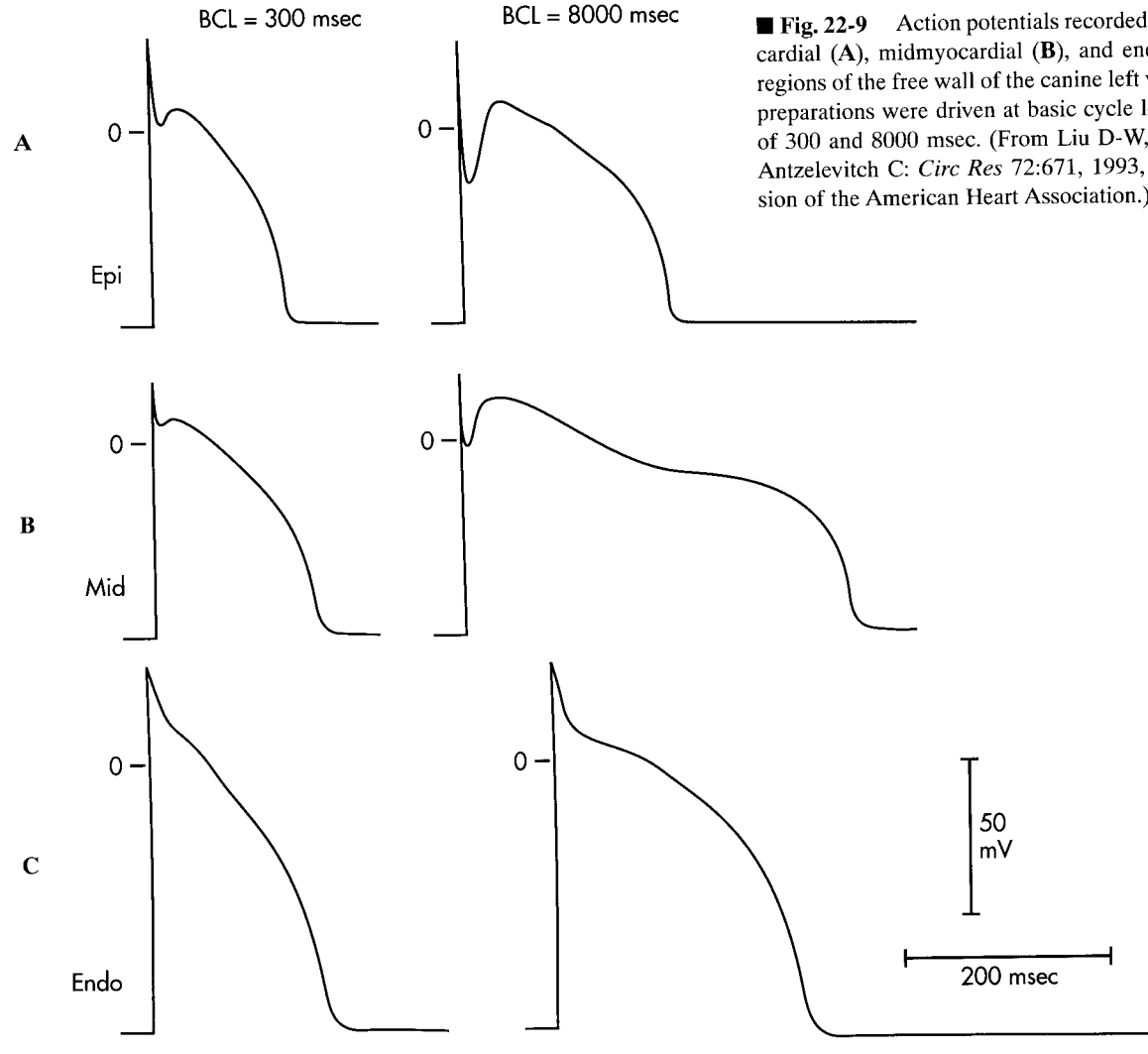

■ **Fig. 22-9** Action potentials recorded from the epicardial (**A**), midmyocardial (**B**), and endocardial (**C**) regions of the free wall of the canine left ventricle. The preparations were driven at basic cycle lengths (*BCL*) of 300 and 8000 msec. (From Liu D-W, Gintant GA, Antzelevitch C: *Circ Res* 72:671, 1993, with permission of the American Heart Association.)

ing the plateau as it is during phase 4, the efflux of K^+ during phase 2 would greatly exceed the influx of Ca^{++}, and a sustained plateau could not be achieved. However as V_m approaches and then attains positive values near the peak of the action potential upstroke, g_K suddenly decreases (Fig. 22-7). *The diminished K^+ current associated with the reduction in g_K prevents an excessive loss of K^+ from the cell during the plateau.*

This reduction in g_K at both positive and low negative values of V_m is called **inward rectification.** Inward rectification is a characteristic of several K^+ currents, including the i_{K1} current. The current-voltage relationship of the K^+ channels that conduct i_{K1} has been determined by voltage-clamping cardiac cells (Fig. 22-12). Note that for the cell depicted in the figure, the current-voltage curve intersects the voltage axis at a V_m of about

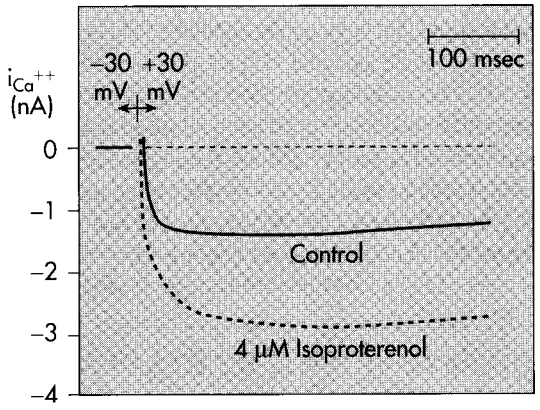

■ **Fig. 22-10** Effect of isoproterenol on the Ca^{++} current conducted by L-type Ca^{++} channels in voltage-clamped, canine atrial myocytes when the potential was changed from −30 to +30 mV. (Redrawn from Bean BP: *J Gen Physiol* 86:1, 1985.)

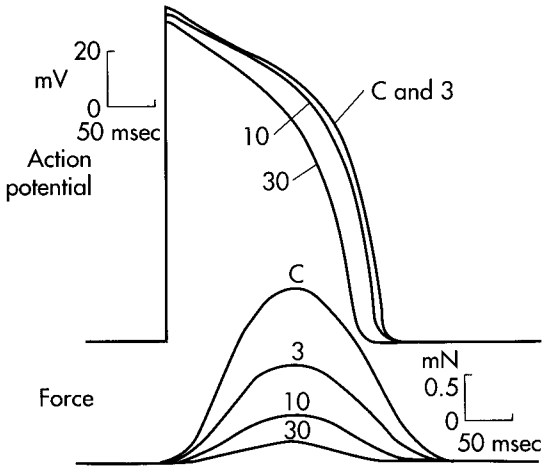

■ **Fig. 22-11** Effects of diltiazem, a Ca^{++} channel antagonist, on the action potentials (in millivolts) and isometric contractile forces (in millinewtons) recorded from an isolated papillary muscle of a guinea pig. The tracings were recorded under control conditions *(C)* and in the presence of diltiazem, in concentrations of 3, 10, and 30 μmol/L. (Redrawn from Hirth C, Borchard U, Hafner D: *J Mol Cell Cardiol* 15:799, 1983.)

−70 mV. The absence of ionic current flow at the point of intersection indicates that the electrostatic forces are equal to the chemical (diffusional) forces (Fig. 22-3) at this potential. In this ventricular cell preparation, therefore, the Nernst equilibrium potential (E_K) for K^+ is −70 mV. This value reflects the ratio of intracellular to extracellular K^+ concentration that prevails in this particular experimental preparation.

When the membrane potential is clamped at levels negative to −70 mV in this same isolated cardiac cell (Fig. 22-12), the electrostatic forces exceed the chemical forces and an inward K^+ current is induced (as denoted by the negative values of K^+ current over this range of voltages). Note also that for V_m more negative than −70 mV, the curve has a steep slope, even at the point of intersection (at which $V_m = E_K$). Thus when V_m equals or is negative to E_K, a small change in V_m induces a substantial change in K^+ current; that is, g_K is large. During phase 4, the V_m of a myocardial cell is slightly less negative than E_K (Fig. 22-4). The substantial g_K that prevails during phase 4 of the cardiac action potential (Fig. 22-7) is accounted for mainly by the i_{K1} channels.

When the transmembrane potential is clamped at levels less negative than −70 mV (Fig. 22-12), the chemical forces exceed the electrostatic forces. Therefore, the net K^+ currents are directed outward (as denoted by the corresponding positive values of K^+ current). Note that for V_m values less negative than −70 mV the curve is relatively flat, and for V_m values less negative than about −30 mV the K^+ current is virtually zero. Thus, at V_m values that prevail during the action potential plateau, the efflux of K^+ through the i_{K1} channels is negligible. Conversely, as we have seen, the inwardly directed K^+ current is sub-

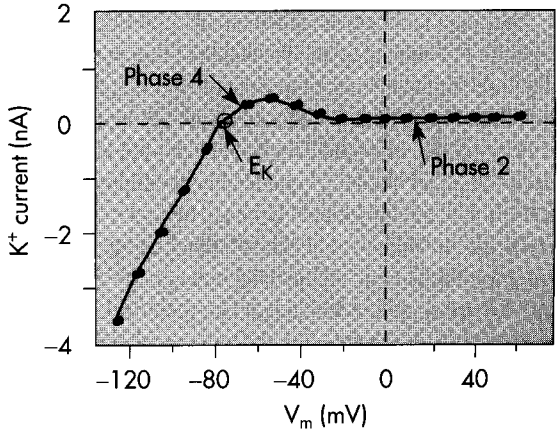

■ **Fig. 22-12** Inwardly rectified K^+ currents recorded from a rabbit ventricular myocyte when the potential was changed from a holding potential of −80 mV to various test potentials. Positive values along the vertical axis represent outward currents; negative values represent inward currents. The V_m coordinate of the point *(open circle)* at which the curve intersects the X axis is the reversal potential; it denotes the Nernst equilibrium potential, at which point the chemical and electrostatic forces are equal. (Redrawn from Giles WR, Imaizumi Y: *J Physiol (Lond)* 405:123, 1988.)

stantial for those values of V_m that prevail during phase 4. Thus, the i_{K1} current is **inwardly rectified.**

The characteristics of another K^+ channel, the **delayed rectifier (i_K)** channel, also contribute to the low g_K that prevails during the plateau. These K^+ channels are closed during phase 4, but they are activated by the potentials that prevail toward the end of phase 0. However, activation proceeds very slowly during the plateau. Hence, activation of these channels tends to increase g_K very gradually during phase 2. Thus, these channels play only a minor role during phase 2, but they do contribute to the process of final repolarization (phase 3), as described below.

The action potential plateau persists as long as the efflux of charge carried mainly by K^+ is balanced by the influx of charge carried mainly by Ca^{++}. The effects of altering this balance are demonstrated by the action of the calcium channel antagonist diltiazem in an isolated papillary muscle preparation. Fig. 22-11 shows that with increasing concentrations of diltiazem, the voltage of the plateau becomes progressively less positive and the duration of the plateau diminishes. Similarly, administration of certain K^+ channel antagonists prolongs the plateau substantially.

■ *Phase 3: Genesis of Final Repolarization*

The process of final repolarization (phase 3) starts at the end of phase 2, when the efflux of K^+ from the cardiac cell begins to exceed the influx of Ca^{++}. As we have noted, at least three outward K^+ currents (i_{to}, i_K, and i_{K1}) contribute to the final repolarization (phase 3) of the cardiac cell (Fig. 22-8).

The transient outward (i_{to}) and the delayed rectifier (i_K) currents help initiate repolarization. These currents are therefore important determinants of the duration of the plateau. For example, the plateau duration is substantially less in atrial than in ventricular myocytes (Fig. 22-19). Electrophysiological experiments reveal that the intensity of the outward K^+ current during the plateau is greater in atrial than in ventricular myocytes. When the outward K^+ current exceeds the inward Ca^{++} current, repolarization begins. Hence, the greater the K^+ current during phase 2, the earlier repolarization begins. The greater density of the K^+ current in atrial than in ventricular myocytes accounts for the shorter action potentials in atrial than in ventricular myocytes.

The action potential duration in ventricular myocytes varies considerably with the locations of these myocytes in the ventricular walls (Fig. 22-9). The delayed rectifier (i_K) current appears to account for these differences. In endocardial myocytes, where the action potential duration is least, the intensity of i_K is greatest. The converse applies to the midmyocardial myocytes. The intensity of i_K and the action potential duration are intermediate for the epicardial myocytes.

The inwardly rectified K^+ current, i_{K1}, does not participate in the initiation of repolarization, because the conductance of these channels is very small at the range of V_m values that prevail during the plateau. However, *the i_{K1} channels do contribute substantially to the rate of repolarization once phase 3 has been initiated.* As the net efflux of cations causes V_m to become increasingly negative during phase 3, the conductance of the channels that carry the i_{K1} current progressively increases. In Fig. 22-12, the hump in the flat portion of the current-voltage curve reflects the increase in i_{K1} conductance as V_m changes from about -20 to about -60 mV. Thus, as V_m passes through this range of values positive to the Nernst equilibrium potential (open circle in Fig. 22-12), the outward K^+ current increases and thereby accelerates repolarization.

■ *Phase 4: Restoration of Ionic Concentrations*

The excess Na^+ that enters the cell rapidly during phase 0 and more slowly throughout the cardiac cycle is eliminated by the action of the enzyme Na^+,K^+-ATPase. This enzyme ejects 3 Na^+ in exchange for 2 K^+ that had exited from the cell mainly during phases 2 and 3. Similarly, most of the excess Ca^{++} that had entered the cell mainly during phase 2 is eliminated principally by a Na^+/Ca^{++} exchanger, which exchanges 3 Na^+ for 1 Ca^{++}. However, some of the Ca^{++} is eliminated by an ATP-driven Ca^{++} pump (Fig. 23-5).

■ *Ionic Basis of the Slow Response*

Fast-response action potentials (Fig. 22-1, *A*) consist of four principal components: an upstroke (phase 0); an early, partial repolarization (phase 1); a plateau (phase 2); and a final repolarization (phase 3). However, in the slow response (Fig. 22-1, *B*), the upstroke is much less steep, early repolarization (phase 1) is absent, the plateau is less prolonged and not as flat, and the transition from the plateau to the final repolarization is less distinct.

Blocking fast Na^+ channels with tetrodotoxin in a fast-response fiber can generate slow responses under appropriate conditions. The Purkinje fiber action potentials shown in Fig. 22-13 clearly exhibit the two response types. In the control tracing (*A*), the typical fast-response action potential displays a prominent notch, which separates the upstroke from the plateau. In action potentials *B* to *E*, progressively larger quantities of tetrodotoxin are added to the bathing solution to produce a graded blockade of the fast Na^+ channels. Fig. 22-13 shows that the upstroke and notch become progressively less prominent in action potentials *B* to *D*. In action potential *E*, the notch has disappeared and the upstroke is very gradual; the action potential resembles a typical slow response.

Certain cells in the heart, notably those in the SA and AV nodes, are normally slow-response fibers. In such fibers, depolarization is achieved mainly by the influx of Ca^{++} through the Ca^{++} channels. Repolarization is accomplished in these fibers by the inactivation of the

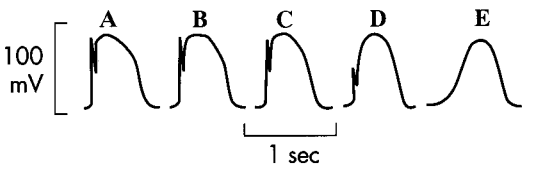

■ **Fig. 22-13** Effect of tetrodotoxin on the action potentials recorded in a calf Purkinje fiber perfused with a solution containing epinephrine and K^+ (10.8 mM). The concentration of tetrodotoxin was 0 M in **A**, 3×10^{-8} M in **B**, 3×10^{-7} M in **C**, and 3×10^{-6} M in **D** and **E**; **E** was recorded later than **D**. (Redrawn from Carmeliet E, Vereecke J: *Pflugers Arch* 313:300, 1969.)

Ca^{++} channels and by the increased K^+ conductance through the i_{K1} and i_K channels (Fig. 22-8).

■ *Conduction in Cardiac Fibers*

Now that we have seen how an action potential is generated, let us turn to how an action potential is conducted in a cardiac fiber. An action potential traveling down a cardiac muscle fiber is propagated by local circuit currents, much as it does in nerve and skeletal muscle fibers (see Chapter 3). The characteristics of conduction differ in fast- and slow-response fibers.

■ *Conduction of the Fast Response*

In fast-response fibers, the fast Na^+ channels are activated when the transmembrane potential of one region of the fiber suddenly changes from a resting value of about −90 mV to the threshold value of about −70 mV. The inward Na^+ current then rapidly depolarizes the cell at that site. This portion of the fiber becomes part of the depolarized zone, and the border is displaced accordingly. The same process then begins at the new border. This process is repeated again and again, and the border moves continuously down the fiber as a wave of depolarization (see Fig. 3-11).

The conduction velocity along the fiber varies directly with the amplitude of the action potential and the rate of change of potential (dV_m/dt) during phase 0. The amplitude of the action potential equals the difference in potential between the fully depolarized and the fully polarized regions of the cell interior. The magnitude of the local currents is proportional to this potential difference (see Chapter 3). Because these local currents shift the potential of the resting zone toward the threshold value, they act as the local stimuli that depolarize the adjacent resting portion of the fiber to its threshold potential. *The greater the potential difference between the depolarized and polarized regions (i.e., the greater the amplitude of the action potential), the more effective are the local stimuli in depolarizing adjacent parts of the membrane and the more rapidly is the wave of depolarization propagated down the fiber.*

The rate of change of potential (dV_m/dt) during phase 0 is also an important determinant of the conduction velocity. If the active portion of the fiber depolarizes gradually, the local currents between the resting region and the neighboring depolarizing region are small. The resting region adjacent to the active zone is depolarized gradually, and consequently more time is required for each new section of the fiber to reach threshold.

The level of the resting membrane potential is also an important determinant of conduction velocity. This factor operates by influencing the amplitude of the action potential and the slope of the upstroke. The transmembrane potential just prior to depolarization may vary for the following reasons: (1) the external K^+ concentration has changed (Fig. 22-4); (2) in cardiac fibers that are intrinsically automatic, V_m becomes progressively less negative during phase 4 (Fig. 22-19, *B*); and (3) if the cell is excited prematurely, the cell membrane has not repolarized fully from the preceding excitation (Fig. 22-15). In general, the less negative the level of V_m, the less is the velocity of impulse propagation, regardless of the reason for the change in V_m.

The V_m level affects conduction velocity because the inactivation, or h, gates (Fig. 22-6) in the fast Na^+ channels are voltage dependent. The less negative the V_m, the greater is the number of h gates that tend to close. During the normal process of excitation, depolarization proceeds so rapidly during phase 0 that the comparatively slow h gates do not close until the end of that phase. However, if partial depolarization is produced by a more gradual process, such as by an elevation of the level of external K^+, the gates have ample time to close and thereby inactivate some of the Na^+ channels. When the cell is partially depolarized, many of the Na^+ channels are already inactivated; thus, only a fraction of the Na^+ channels is available to conduct the inward Na^+ current during phase 0.

Fig. 22-14 shows the results of an experiment in which the resting V_m of a bundle of Purkinje fibers is closed by altering the value of $[K^+]_o$. When $[K^+]_o$ is 3 mM (*A* and *F*), the resting V_m is −82 mV and the slope of phase 0 is steep. At the end of phase 0, the overshoot attains a value of 30 mV. Hence, the amplitude of the action potential is 112 mV. The tissue is stimulated at some distance from the impaled cell, and the stimulus artifact (*St*) appears as a diphasic deflection just before phase 0. The distance from this artifact to the beginning of phase 0 is inversely proportional to the conduction velocity.

When $[K^+]_o$ is increased gradually to 16 mM (*B* to *E*), the resting V_m becomes progressively less negative. At the same time, the amplitudes and durations of the action potentials and the steepness of the upstrokes all diminish. As a consequence, the conduction velocity diminishes progressively. At $[K^+]_o$ levels of 14 and 16 mM (*D* and *E*), the resting V_m attains levels sufficient to inactivate all the fast Na^+ channels. The action potentials in panels *D* and *E* are characteristic slow responses.

■ *Slow Response*

In slow-response fibers, the relative refractory period frequently extends well beyond phase 3 (Fig. 22-1, *B*). Even after the cell has completely repolarized, it may be difficult to evoke a propagated response for some time. This characteristic of slow-response fibers is called **post-repolarization refractoriness.**

Action potentials evoked early in the relative refractory period are small and the upstrokes are not very steep (Fig. 22-16). The amplitudes and upstroke slopes progressively improve as action potentials are elicited later in the relative refractory period. The recovery of full excitability is much slower than in the fast response. Impulses that arrive early in the relative refractory period are conducted much more slowly than those that arrive late in that period. The lengthy refractory periods also lead to conduction blocks. Even when slow responses recur at a low repetition rate, the fiber may be able to conduct only a fraction of those impulses; for example, only alternate impulses may be propagated (Fig. 22-38, *B*).

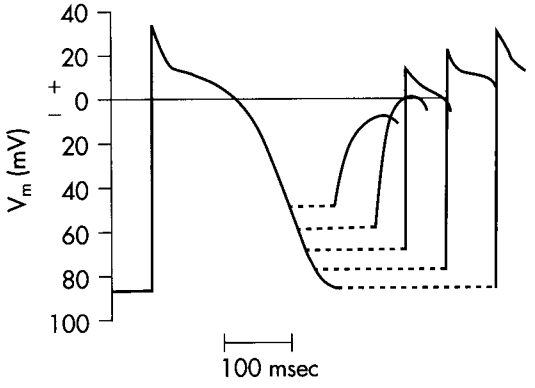

■ **Fig. 22-15** The changes in action potential amplitude and upstroke slope as action potentials are initiated at different stages of the relative refractory period of the preceding excitation. (Redrawn from Rosen MR, Wit AL, Hoffman BF: *Am Heart J* 88:380, 1974.)

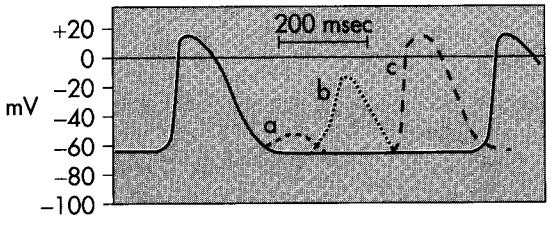

■ **Fig. 22-16** Effects of excitation at various times after the initiation of an action potential in a slow-response fiber. In this fiber, excitation very late in phase 3 (or early in phase 4) induces a small, nonpropagated (local) response *(a)*. Later in phase 4, a propagated response *(b)* can be elicited, but its amplitude is small and the upstroke is not very steep; this response is conducted very slowly. Still later in phase 4, full excitability is regained, and the response *(c)* displays normal characteristics. (Modified from Singer DH et al: *Prog Cardiovasc Dis* 24:97, 1981.)

■ *Effects of Cycle Length*

Changes in cycle length alter the duration of action potentials in cardiac cells (Figs. 22-9 and 22-17) and thus change their refractory periods. Consequently, changes in cycle length are often important factors in the initiation or termination of certain arrhythmias (irregular heat rhythms). The changes in action potential durations produced by stepwise reductions in cycle length from 2000 to 200 msec in a Purkinje fiber are shown in Fig. 22-17. Note that as the cycle length diminishes, the action potential duration decreases. The direct correlation between action potential duration and cycle length is mediated by changes in g_K that involve at least two types of K^+ channels, namely, those that conduct the delayed rectifier K^+ current, i_K, and those that conduct the transient outward K^+ current, i_{to}.

The i_K current is activated at values of V_m near zero, but the current activates slowly and remains activated for hundreds of milliseconds. The i_K current also inactivates very slowly. Consequently, as the basic cycle length diminishes, each action potential tends to occur earlier in the inactivation period of the i_K current of the preceding action potential. Therefore, the shorter the basic cycle length, the greater is the outward K^+ current during phase 2, and hence the shorter the duration of the action potential.

The i_{to} current also influences the relationship between cycle length and action potential duration. The i_{to} current is also activated at near zero potentials, and its magnitude varies inversely with the cardiac cycle length. Therefore, as cycle length decreases, the resultant increase in the outward K^+ current shortens the plateau. The relative

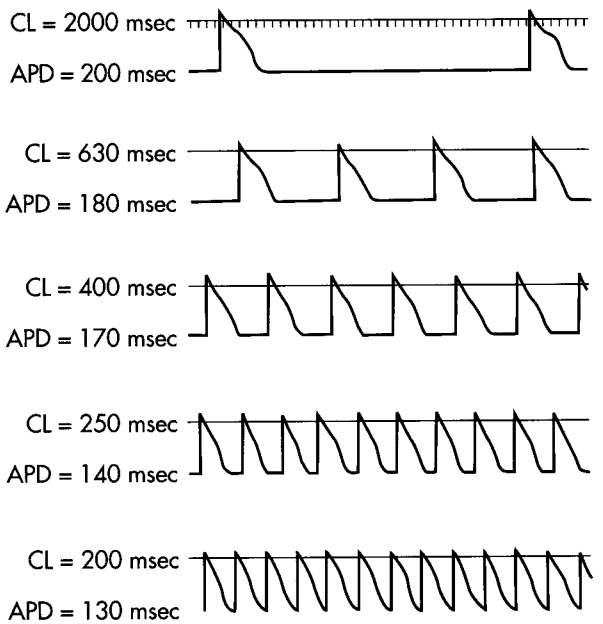

■ **Fig. 22-17** Effect of changes in cycle length *(CL)* on the action potential duration *(APD)* of canine Purkinje fibers. (Modified from Singer D, Ten Eick RE: *Am J Cardiol* 28:381, 1971.)

contributions of i_K and of i_{to} to the relationship between action potential duration and cardiac cycle length vary from species to species.

■ *Natural Excitation of the Heart*

The nervous system controls various aspects of cardiac behavior, such as the heart rate and the strength of each contraction. However, cardiac function does not require an intact innervation. Indeed, a cardiac transplant patient, whose heart is completely denervated, can adapt well to stressful situations. The ability of the denervated, transplanted heart to function and adapt to changing conditions lies in certain intrinsic properties of cardiac tissue, especially its automaticity.

The properties of ***automaticity*** *(the ability to initiate its own beat) and* ***rhythmicity*** *(the regularity of such pacemaking activity) allow the heart to beat even when it is completely removed from the body.* If the coronary vasculature of an excised heart is artificially perfused with blood or an oxygenated electrolyte solution, rhythmic cardiac contractions persist for many hours. At least some cells in the atria and ventricles can initiate beats; such cells mainly reside in the nodal tissues or specialized conducting fibers of the heart.

The region of the mammalian heart that ordinarily generates impulses at the greatest frequency is the **sinoatrial (SA) node;** it is the main **pacemaker** of the heart. Detailed mapping of the electrical potentials on the surface of the right atrium reveals that two or three sites of automaticity, located 1 or 2 cm from the SA node itself, serve along with the SA node as an **atrial pacemaker complex.** At times, all of these loci initiate impulses simultaneously. At other times, the site of earliest excitation shifts from locus to locus, depending on certain conditions, such as the level of autonomic neural activity.

Regions of the heart other than the SA node may initiate beats under special circumstances. Such sites are called **ectopic foci,** or **ectopic pacemakers.** Ectopic foci may become pacemakers when (1) their own rhythmicity becomes enhanced, (2) the rhythmicity of the higher-order pacemakers becomes depressed, or (3) all conduction pathways between the ectopic focus and those regions with greater rhythmicity become blocked. Ectopic pacemakers may act as a safety mechanism when normal pacemaking centers fail. However, if an ectopic center fires while the normal pacemaking center still functions, the ectopic activity may induce either sporadic rhythm disturbances, such as **premature depolarizations** (Fig. 22-39), or continuous rhythm disturbances, such as **paroxysmal tachycardias** (Fig. 22-40).

When the SA node or other components of the atrial pacemaker complex are excised or destroyed, pacemaker cells in the AV junction usually take over the pacemaker function for the entire heart. After some time, which may vary from minutes to days, automatic cells in the atria usually become dominant. Purkinje fibers in the specialized conduction system of the ventricles also display automaticity. Characteristically, these fibers fire at a very slow rate. When the AV junction cannot conduct cardiac impulses from the atria to the ventricles (Fig. 22-38, *C*), these **idioventricular pacemakers** in the Purkinje fiber network initiate the ventricular contractions, but at a frequency of only 30 to 40 beats/min.

■ *Sinoatrial Node*

In humans, the SA node is about 8 mm long and 2 mm thick and lies posteriorly in the groove at the junction between the superior vena cava and the right atrium (Fig. 22-18). The sinus node artery runs lengthwise through the center of the node. The SA node contains two principal types of cells: (1) small, round cells, which have few organelles and myofibrils; and (2) slender, elongated cells, which are intermediate in appearance between the round and "ordinary" atrial myocardial cells. The round cells are probably the pacemaker cells, whereas the slender, elongated cells probably conduct the impulses within the node and to the nodal margins.

A typical transmembrane action potential recorded from a cell in the SA node is depicted in Fig. 22-19, *B*. Compared with the transmembrane potential recorded from a ventricular myocardial cell (Fig. 22-19, *A*), the resting potential of the SA node cell is usually less negative, the upstroke of the action potential (phase 0) is less steep, a plateau is not sustained, and repolarization (phase 3) is more gradual. These attributes are all characteristic of the slow response. Again, as in cells that exhibit the slow response, tetrodotoxin has no influence on the SA nodal action potential. Thus, the upstroke of the action potential is not produced by an inward current of Na^+ through fast channels.

The transmembrane potential during phase 4 is much less negative in SA (and AV) nodal automatic cells than in atrial or ventricular myocytes because the i_{K1} (inward

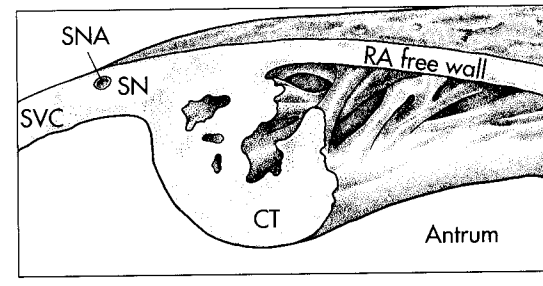

■ **Fig. 22-18** Location of the sinoatrial (SA) node near the junction between the superior vena cava (*SVC*) and the right atrium (*RA*). *SN,* SA node; *SNA,* sinoatrial artery; *CT,* crista terminalis. (Redrawn from James TN: *Am J Cardiol* 40:965, 1977.)

rectifying) type of K^+ channel is sparse in the nodal cells. Therefore, the ratio of g_K to g_{Na} during phase 4 is much less in the nodal cells than in the myocytes. Hence, during phase 4, V_m deviates much more from the K^+ equilibrium potential (E_K) in nodal cells than it does in myocytes.

However, the principal feature of a pacemaker fiber that distinguishes it from the other fibers we have discussed resides in phase 4. In nonautomatic cells, the potential remains constant during this phase, whereas *a pacemaker fiber is characterized by a slow diastolic depolarization throughout phase 4.* Depolarization proceeds at a steady rate until a threshold is attained, triggering an action potential.

The discharge frequency of pacemaker cells may be varied by a change in (1) the rate of depolarization during phase 4, (2) the maximal negativity during phase 4, or (3) the threshold potential (Fig. 22-20). When the rate of slow diastolic depolarization is increased (from *b* to *a* in Fig. 22-20, *A*), the threshold potential is attained earlier, and the heart rate increases. A rise in the threshold potential (from TP-1 to TP-2 in Fig. 22-20, *B*) delays the onset of phase 0 (from time *b* to time *c*), and the heart rate is reduced accordingly. Similarly, when the maximal negative potential is increased (from *a* to *d* in Fig. 22-20, *B*), more time is required to reach threshold TP-2 when the slope of phase 4 remains unchanged, and the heart rate therefore diminishes.

Ordinarily, the frequency of pacemaker firing is controlled by the activity of both divisions of the autonomic nervous system. Increased sympathetic nervous activity, through the release of norepinephrine, raises the heart rate principally by increasing the slope of the slow diastolic depolarization. This mechanism of increasing heart rate occurs during physical exertion, anxiety, or certain illnesses, such as **febrile infectious diseases.**

Increased vagal activity, through the release of acetylcholine, diminishes the heart rate by hyperpolarizing the pacemaker cell membrane and reducing the slope of the slow diastolic depolarization (Fig. 22-21). These mechanisms of decreasing heart rate occur when vagal activity is predominant. An extreme example is **vasovagal syncope,** a brief period of lightheadedness or loss of consciousness caused by an intense burst of vagal activity. This type of syncope is a reflex response to pain or certain psychological stimuli.

Changes in autonomic neural activity usually do not change heart rate by altering the threshold level of V_m that initiates the firing of a nodal pacemaker cell. However, certain antiarrhythmic drugs, such as **quinidine** and **procainamide,** do raise the threshold potential of the automatic cells to less negative values.

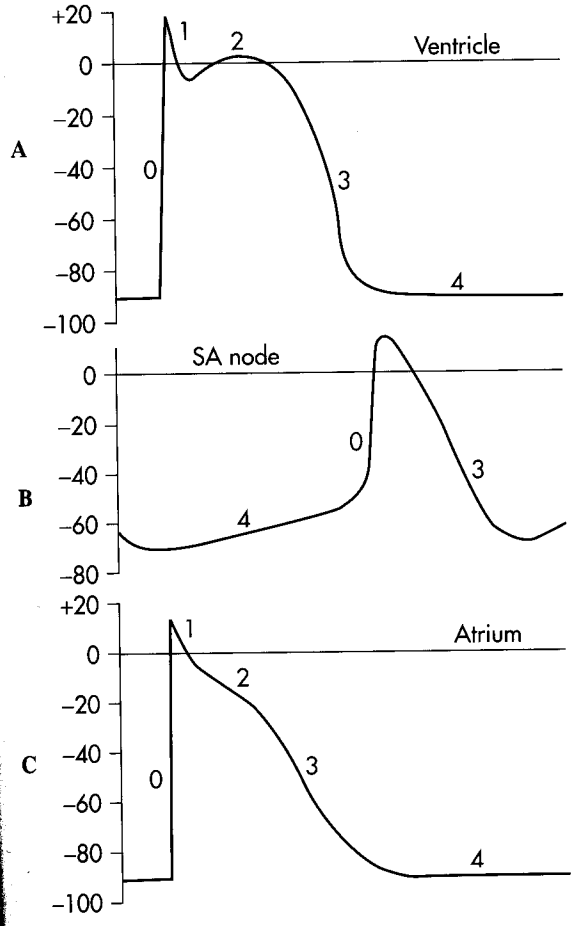

■ **Fig. 22-19** Typical action potentials (in millivolts) recorded from cells in the ventricle **(A),** SA node **(B),** and atrium **(C).** Sweep velocity in **B** is one half that in **A** or **C.** (From Hoffman BF, Cranefield PF: *Electrophysiology of the heart,* New York, 1960, McGraw-Hill.)

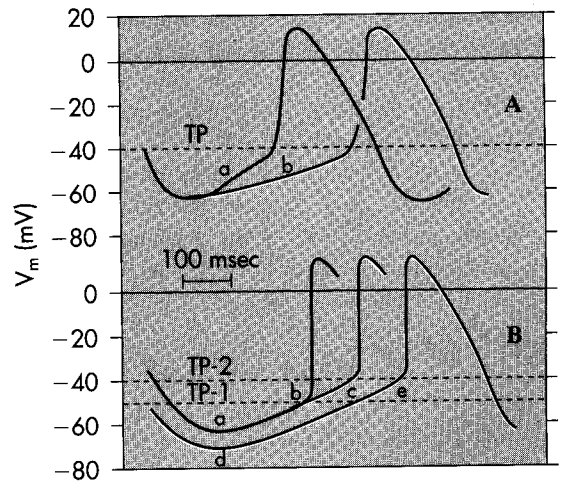

■ **Fig. 22-20** Mechanisms involved in the changes in frequency of pacemaker firing. In **A,** a reduction in the slope (from *a* to *b*) of slow diastolic depolarization diminishes the firing frequency. In **B,** an increase in the threshold potential (from *TP-1* to *TP-2*) or an increase in the magnitude of the resting potential (from *a* to *d*) also diminishes the firing frequency. (Redrawn from Hoffman BF, Cranefield PF: *Electrophysiology of the heart,* New York, 1960, McGraw-Hill.)

Ionic basis of automaticity. Several ionic currents contribute to the slow diastolic depolarization that characteristically occurs in the automatic cells in the heart. In the pacemaker cells of the SA node, at least three ionic currents mediate the slow diastolic depolarization: (1) an inward current, i_f, induced by hyperpolarization; (2) an inward Ca^{++} current, i_{Ca}; and (3) an outward K^+ current, i_K (Fig. 22-22).

The inward current, i_f, is activated near the end of repolarization. This "funny" current is carried mainly by Na^+ through specific channels that differ from the fast Na^+ channels. The current was dubbed "funny" because its discoverers had not expected to detect an inward Na^+ current in pacemaker cells after completion of repolarization. This current is activated as the membrane potential becomes more negative than about −50 mV. The more negative the membrane potential at this time, the greater is the activation of the i_f current.

The second current responsible for diastolic depolarization is the Ca^{++} current, i_{Ca}. This current is activated toward the end of phase 4, as the transmembrane potential reaches a value of about −55 mV (Fig. 22-22). Once the Ca^{++} channels are activated, influx of Ca^{++} into the cell increases. This influx accelerates the rate of diastolic depolarization, which then leads to the upstroke of the action potential. A decrease in the external Ca^{++} concentration (Fig. 22-23) or the addition of calcium channel antagonists (Fig. 22-24) diminishes the amplitude of the action potential and the slope of the slow diastolic depolarization in SA node cells.

The progressive diastolic depolarization mediated by the two inward currents, i_f and i_{Ca}, is opposed by an outward current, the delayed rectifier K^+ current, i_K. This efflux of K^+ tends to repolarize the cell after the upstroke of the action potential. K^+ continues to move out well beyond the time of maximal repolarization, but it diminishes throughout phase 4 (Fig. 22-22). As the current diminishes, its opposition to the depolarizing effects of the two inward currents (i_{Ca} and i_f) also gradually decreases.

The ionic basis for automaticity in the AV node pacemaker cells resembles that in the SA node cells. Similar mechanisms also account for automaticity in ventricular Purkinje fibers, except that the Ca^{++} current is not involved. In other words, the slow diastolic depolarization is mediated principally by the imbalance between the effects of the hyperpolarization-induced inward current, i_f, and the gradually diminishing outward K^+ current, i_K.

The autonomic neurotransmitters affect automaticity by altering the ionic currents across the cell membranes. The adrenergic transmitters increase all three currents involved in SA nodal automaticity. To increase the slope of diastolic depolarization, the augmentations of i_f and

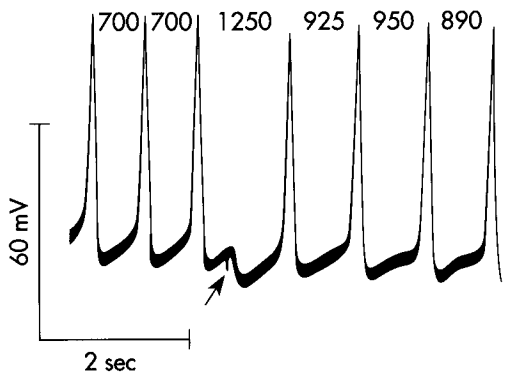

■ **Fig. 22-21** Effect of a brief vagal stimulus *(arrow)* on the transmembrane potential recorded from an SA node pacemaker cell in an isolated cat atrium preparation. The cardiac cycle lengths, in milliseconds, are denoted by the numbers at the top of the figure. (Modified from Jalife J, Moe GK: *Circ Res* 45:595, 1979, with permission of the American Heart Association.)

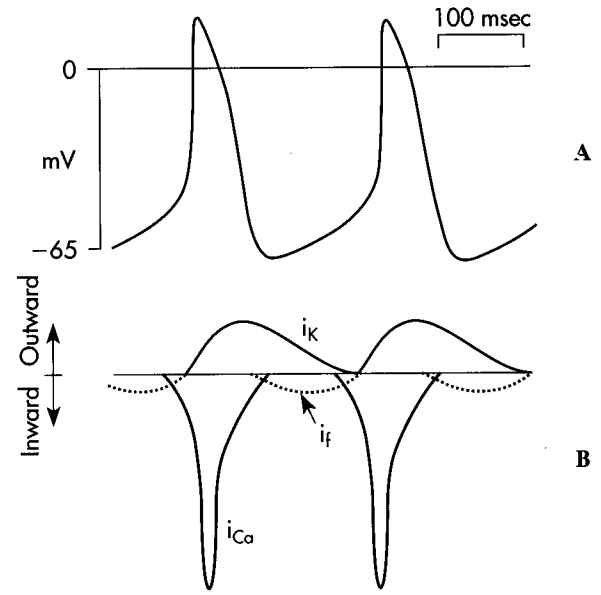

■ **Fig. 22-22** The transmembrane potential changes **(A)** that occur in SA node cells are produced by three principal currents **(B):** (1) an inward Ca^{++} current, i_{Ca}; (2) a hyperpolarization-induced inward current, i_f; and (3) an outward K^+ current, i_K.

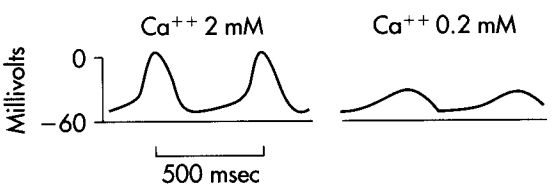

■ **Fig. 22-23** Transmembrane action potentials recorded from an SA node pacemaker cell in an isolated rabbit atrium preparation. The concentration of Ca^{++} in the bath was reduced from 2 mM to 0.2 mM. (Modified from Kohlhardt M, Figulla HR, Tripathi O: *Basic Res Cardiol* 71:17, 1976.)

i_{Ca} by the adrenergic transmitters must exceed the enhancement of i_K.

The hyperpolarization (Fig. 22-21) induced by the acetylcholine released at the vagus endings in the heart is achieved by an increase in g_K. This change in conductance is mediated through activation of specific K^+ channels, the **acetylcholine-regulated K^+** channels. Acetylcholine also depresses the i_f and i_{Ca} currents. The autonomic neural effects on cardiac cells are described in greater detail in Chapter 24.

Overdrive suppression. The automaticity of pacemaker cells diminishes after a period of excitation at a high frequency. This phenomenon is known as **overdrive suppression.** Because the intrinsic rhythmicity of the SA node is greater than that of the other latent pacemaking sites in the heart, the firing of the SA node tends to suppress the automaticity in the other loci.

If an ectopic focus in one of the atria suddenly began to fire at a high rate (e.g., 150 impulses/min) in an individual with a normal heart rate of 70 beats/min, the ectopic site would become the pacemaker for the entire heart. When that rapid ectopic focus suddenly stopped firing, the SA node might remain briefly quiescent because of overdrive suppression. The interval from the end of the period of overdrive until the SA node resumes firing is called the **sinus node recovery time.** In patients with **sick sinus syndrome,** the sinus node recovery time is prolonged. The resultant period of **asystole** (absence of a heartbeat) may cause the patient to lose consciousness.

Overdrive suppression results from the activity of the membrane pump, Na^+, K^+-ATPase, which extrudes 3 Na^+ from the cell in exchange for 2 K^+. Normally, a certain amount of Na^+ enters the cardiac cell during each depolarization. The more frequently the cell is depolarized, therefore, the more Na^+ enters the cell per minute. At high excitation frequencies, the activity of the Na^+, K^+-ATPase increases to extrude this larger amount of Na^+ from the cell interior. Because the amount of Na^+ extruded by the pump exceeds the amount of K^+ that enters the cell, the activity of the Na^+, K^+-ATPase hyperpolarizes the cell. Therefore, the slow diastolic depolarization requires more time to reach the firing threshold, as shown in Fig. 22-20, *B*. Furthermore, when the overdrive suddenly ceases, the activity of the Na^+, K^+-ATPase does not slow down instantaneously but temporarily remains overactive. This excessive extrusion of Na^+ opposes the gradual depolarization of the pacemaker cell during phase 4, and thereby suppresses the cell's intrinsic automaticity transiently.

■ *Atrial Conduction*

From the SA node, the cardiac impulse spreads radially throughout the right atrium (Fig. 22-25) along ordinary atrial myocardial fibers, at a conduction velocity of approximately 1 m/sec. A special pathway, the anterior interatrial myocardial band (or Bachmann's bundle), conducts the impulse from the SA node directly to the left atrium. The wave of excitation that proceeds inferiorly through the right atrium ultimately reaches the AV node, which is normally the sole route of entry of the cardiac impulse to the ventricles.

The configuration of the atrial transmembrane potential is depicted in Fig. 22-19, *C*. Compared with the potential recorded from a typical ventricular fiber (Fig. 22-19, *A*), the atrial plateau (phase 2) is briefer and less developed, and repolarization (phase 3) is slower. The action potential duration in atrial myocytes is shorter than that in ventricular myocytes because the efflux of K^+ is greater during the plateau in atrial myocytes than in ventricular myocytes.

■ *Atrioventricular Conduction*

The atrial excitation wave reaches the ventricles via the AV node. In adult humans, this node is approximately 22 mm long, 10 mm wide, and 3 mm thick. The node is situated posteriorly on the right side of the interatrial septum near the ostium of the coronary sinus. The AV node contains the same two cell types as the SA node, but the round cells in the AV node are less abundant and the elongated cells predominate.

The AV node is made up of three functional regions: (1) the AN region, the transitional zone between the atrium and the remainder of the node; (2) the N region,

■ **Fig. 22-24** Effects of nifedipine (5.6×10^{-7} M), a Ca^{++} channel antagonist, on the transmembrane potentials recorded from an SA node cell in a rabbit. (From Ning W, Wit AL: *Am Heart J* 106:345, 1983.)

the midportion of the AV node; and (3) the NH region, the zone in which nodal fibers gradually merge with the bundle of His, which is the upper portion of the specialized conducting system for the ventricles. Normally, the AV node and bundle of His are the only pathways along which the cardiac impulse travels from atria to ventricles.

Some people have accessory AV pathways. Because these pathways often serve as a part of a reentry loop (Fig. 22-30), they can be associated with serious cardiac rhythm disturbances. **Wolff-Parkinson-White syndrome,** a congenital disturbance, is the most common clinical disorder in which a bypass tract of myocardial fibers serves as an accessory pathway between atria and ventricles. Ordinarily, the syndrome causes no functional abnormality. The disturbance is easily detected in the electrocardiogram (ECG) because a portion of the ventricular myocardium is excited via the bypass tract before the remainder of the ventricular myocardium is excited via the AV node and His-Purkinje system. This preexcitation can be seen as a bizarre configuration in the ventricular (QRS) complex of the ECG. Occasionally, however, a reentry loop develops in which the atrial impulse travels to the ventricles via one of the two AV pathways (AV node or bypass tract), and then back to the atria through the other of the two pathways. Continuous circling around the loop leads to a very rapid rhythm **(supraventricular tachycardia).** This rapid rhythm may be incapacitating because it may not allow sufficient time for ventricular filling. Transient block of the AV node by injecting adenosine intravenously or by increasing vagal activity reflexly (by pressing on the neck over the carotid sinus region) usually abolishes the tachycardia and restores a normal sinus rhythm.

Several features of AV conduction are of physiological and clinical significance. The principal delay in the passage of the impulse from the atria to the ventricles occurs in the AN and N regions of the AV node. The conduction velocity is actually less in the N region than in the AN region. However, the path length is substantially greater in the AN than in the N region. The conduction times through the AN and N zones account for the delay between the start of the **P wave** (the electrical manifestation of the spread of atrial excitation) and the **QRS complex** (spread of ventricular excitation) on an ECG (Fig. 22-33). *Functionally, the delay between atrial and ventricular excitation permits optimal ventricular filling during atrial contraction.*

In the N region, slow-response action potentials prevail. The resting potential is about −60 mV, the upstroke velocity is low (about 5 V/sec), and the conduction velocity is about 0.05 m/sec. Tetrodotoxin, which blocks the fast Na^+ channels, has virtually no effect on the action potentials in this region (or on any other slow-response fibers). Conversely, Ca^{++} channel antagonists decrease the amplitude and duration of the action potentials (Fig. 22-26) and depress AV conduction. The shapes of the action potentials in the AN region are intermediate between those in the N region and atria. Similarly, the action potentials in the NH region are transitional between those in the N region and bundle of His.

Like other slow-response action potentials, the relative refractory period of cells in the N region extends well beyond the period of complete repolarization; that is, these cells display postrepolarization refractoriness (Fig. 22-16). As the time between successive atrial depolarizations is decreased, conduction through the AV junction slows (Fig. 22-27). An abnormal prolongation of the AV conduction time is called **first-degree AV block** (Fig.

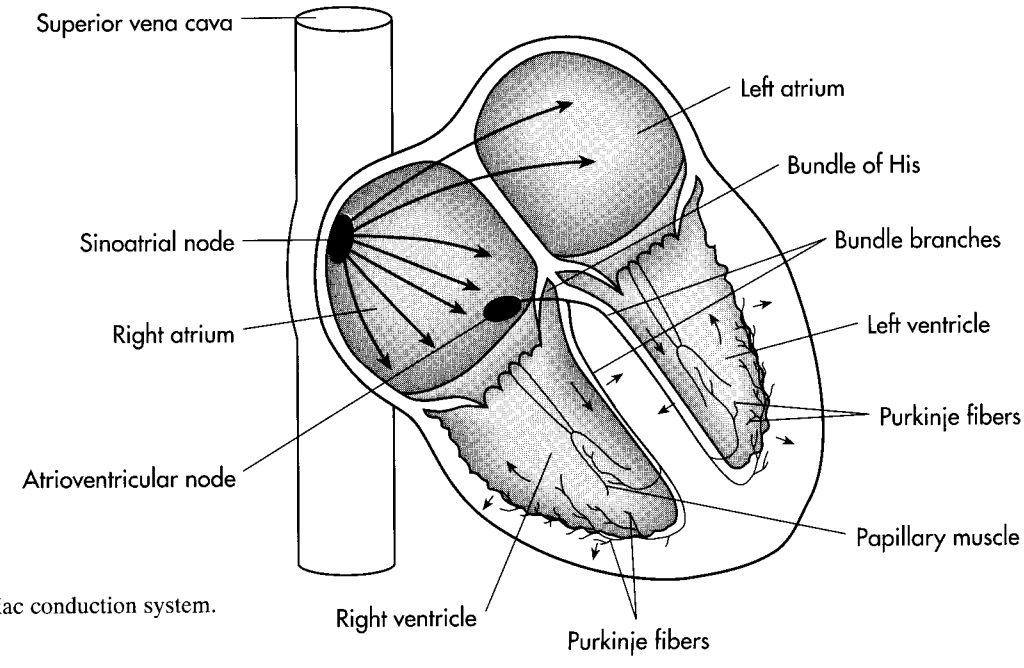

■ **Fig. 22-25** The cardiac conduction system.

22-38, *A*). Most of the prolongation of AV conduction induced by a decrease in atrial cycle length takes place in the N region of the AV node.

Impulses tend to be blocked in the AV node at stimulation frequencies that are easily conducted in other regions of the heart. If the atria are depolarized at a high repetition rate, only a fraction (e.g., one half) of the atrial impulses might be conducted through the AV junction to the ventricles. The conduction pattern in which only a fraction of the atrial impulses are conducted to the ventricles is called **second-degree AV block** (Fig. 22-38, *B*). This type of block may protect the ventricles from excessive contraction frequencies, wherein the filling time between contractions might be inadequate.

Retrograde conduction can occur through the AV node. However, the propagation time is significantly longer and the impulse is blocked at lower repetition rates when the impulse is conducted in the retrograde instead of in the antegrade direction. Finally the AV node is a common site for reentry; the underlying mechanisms are explained on p 349.

The autonomic nervous system regulates AV conduction. Weak vagal activity may simply prolong the AV conduction time. Thus, for any given atrial cycle length, the atrium to His (A-H) or atrium to ventricle (A-V) conduction time will be prolonged by vagal stimulation (Fig. 22-27). Stronger vagal activity may cause some or all of the impulses arriving from the atria to be blocked in the node. The conduction pattern in which none of the atrial impulses reach the ventricles is called **third-degree,** or **complete, AV block** (Fig. 22-38, *C*). The vagally induced delay or absence of conduction through the A-V junction occurs mainly in the N region of the node.

Acetylcholine released by the vagal nerve fibers hyperpolarizes the conducting fibers in the N region (Fig. 22-28). The greater the hyperpolarization at the time of arrival of the atrial impulse, the more impaired is the AV conduction. In the experiment shown in Fig. 22-28, vagus nerve fibers are stimulated intensely (at *St*) shortly before the second atrial depolarization (A_2). That atrial impulse arrives at the AV node cell when its cell membrane is maximally hyperpolarized in response to the vagal stimulus. The absence of a corresponding depolarization of the bundle of His shows that the vagal stimulus prevents the conduction of the second atrial impulse through the AV node. Only a small, nonpropagated response to the second atrial impulse is evident in the recording from the conducting fiber.

The cardiac sympathetic nerves, on the other hand, facilitate AV conduction. They decrease the AV conduction

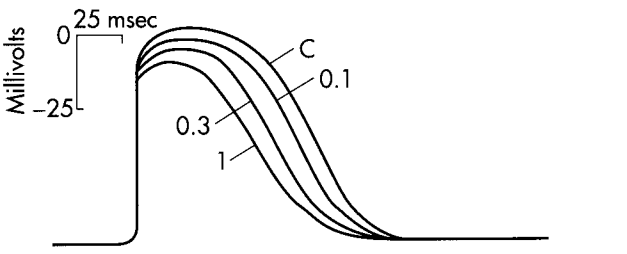

■ **Fig. 22-26** Transmembrane potentials recorded from a rabbit atrioventricular (AV) node cell under control conditions *(C)* and in the presence of the calcium channel antagonist diltiazem, in concentrations of 0.1, 0.3, and 1 μmol/L. (Redrawn from Hirth C, Borchard U, Hafner D: *J Mol Cell Cardiol* 15:799, 1983.)

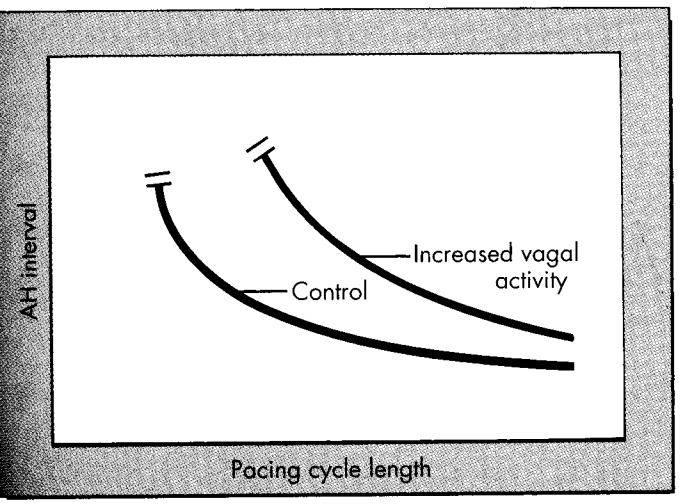

■ **Fig. 22-27** Changes in atrium-His *(AH)* intervals induced by pacing the atria at various cycle lengths in a group of human subjects under control conditions and during a reflexly induced increase in vagal activity produced by the intravenous infusion of phenylephrine. (Redrawn from Page RL et al: *Circ Res*, 68:1614, 1991, with permission of the American Heart Association.)

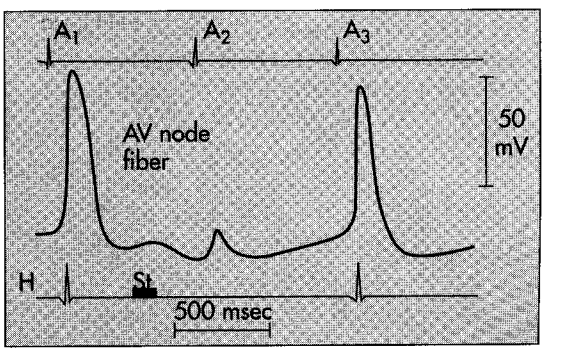

■ **Fig. 22-28** Effects of a brief vagal stimulus *(St)* on the transmembrane potential recorded from an AV nodal fiber from a rabbit. Note that shortly after vagal stimulation, the membrane of the fiber was hyperpolarized. The atrial excitation (A_2) that arrived at the AV node when the cell was hyperpolarized failed to be conducted, as denoted by the absence of a depolarization in the His electrogram *(H)*. The atrial excitations that preceded (A_1) and followed (A_3) excitation A_2 were conducted to the His bundle region. (Redrawn from Mazgalev T et al: *Am J Physiol* 251:H631, 1986.)

time and enhance the rhythmicity of the latent pacemakers in the AV junction. The norepinephrine released at the sympathetic nerve terminals increases the amplitude and slope of the upstroke of the AV nodal action potentials, principally in the AN and N regions of the node.

■ *Ventricular Conduction*

The bundle of His passes subendocardially down the right side of the interventricular septum for about 1 cm and then divides into the right and left **bundle branches** (Figs. 22-25 and 22-29). The right bundle branch, which is a direct continuation of the bundle of His, proceeds down the right side of the interventricular septum. The left bundle branch, which is considerably thicker than the right, arises almost perpendicularly from the bundle of His and perforates the interventricular septum. On the subendocardial surface of the left side of the interventricular septum, the left bundle branch splits into a thin anterior division and a thick posterior division.

Impulse conduction in the right or left bundle branch or in either division of the left bundle branch may be impaired. Conduction blocks may develop in one or more of these conduction pathways as a consequence of **coronary artery disease** or degenerative processes associated with aging, and they give rise to characteristic ECG patterns. Block of either of the main bundle branches is known as right or left **bundle branch block.** Block of either division of the left bundle branch is called left anterior or left posterior **hemiblock.**

The right bundle branch and the two divisions of the left bundle branch ultimately subdivide into a complex network of conducting fibers, called **Purkinje fibers,** which spread out over the subendocardial surfaces of both ventricles. In certain mammalian species, such as cattle, the Purkinje fiber network is arranged in discrete, encapsulated bundles (Fig. 22-29).

Purkinje fibers have abundant, linearly arranged sarcomeres, as do myocytes. However, the T-tubular system is absent in the Purkinje fibers of many species, although it is well developed in the myocytes. Purkinje fibers are the broadest cells in the heart: they are 70 to 80 μm in diameter, compared with diameters of 10 to 15 μm for ventricular myocytes. Partly because of their large diameter, conduction velocity (1 to 4 m/sec) in the Purkinje fibers exceeds that of any other fiber type within the heart. The increased conduction velocity permits a rapid activation of the entire endocardial surface of the ventricles.

The action potentials recorded from Purkinje fibers resemble those of ordinary ventricular myocardial fibers (Figs. 22-9 and 22-19, *A*). In general, phase 1 is prominent in Purkinje fiber action potentials (Fig. 22-13) and the duration of the plateau (phase 2) is intermediate between those of epicardial and midmyocardial myocytes (Fig. 22-9).

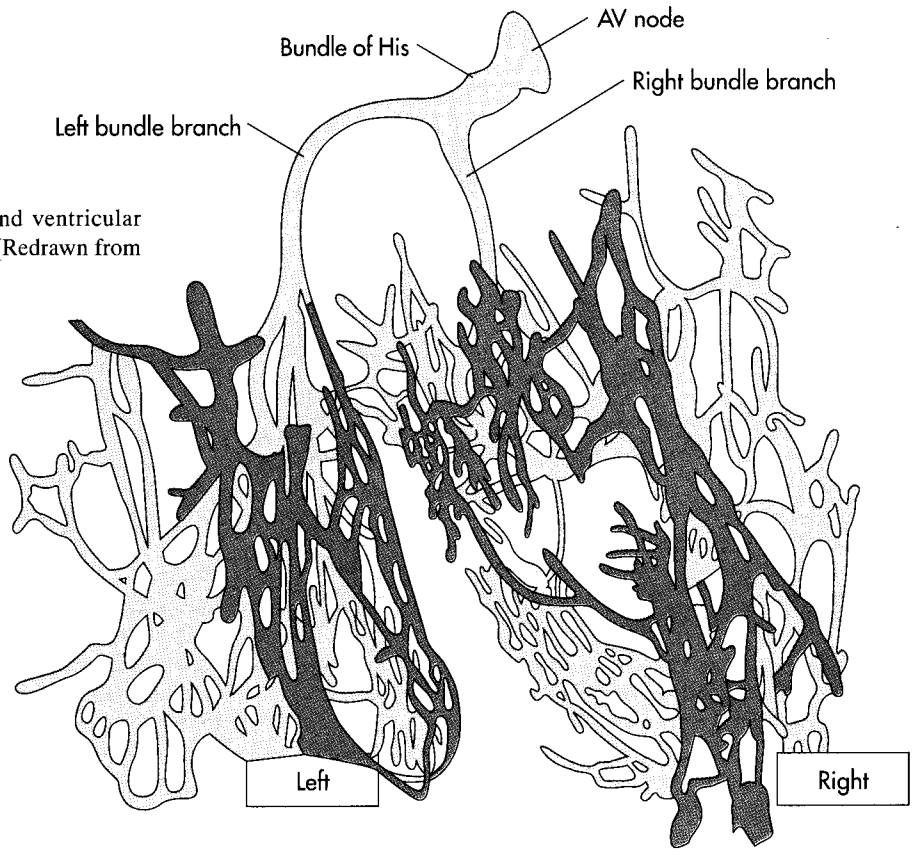

■ **Fig. 22-29** Atrioventricular and ventricular conduction system of the calf heart. (Redrawn from DeWitt LM: *Anat Rec* 3:475, 1909.)

Because of the long refractory period of Purkinje fiber action potentials, many premature excitations of the atria are conducted through the AV junction but are blocked by the Purkinje fibers. Blockage of these atrial excitations prevents premature contraction of the ventricles. This function of protecting the ventricles against the effects of premature atrial depolarizations is especially pronounced at slow heart rates, because the action potential duration, and hence the effective refractory period of the Purkinje fibers, varies inversely with the heart rate (Fig. 22-17). At slow heart rates, the effective refractory period of the Purkinje fibers is especially prolonged; as the heart rate increases, the refractory period diminishes. Similar directional changes in the refractory period occur also in ventricular myocytes in response to changes in rate (Fig. 22-9). However, in the AV node, the effective refractory period does not change appreciably over the normal range of heart rates, and it actually increases at very rapid heart rates (Fig. 22-27). Therefore, *when the atrium is excited at high repetition rates, it is the AV node that protects the ventricles from these excessively high frequencies.*

The first portions of the ventricles to be excited by impulses arriving from the AV node are the interventricular septum (except the basal portion) and the papillary muscles. The wave of activation spreads into the substance of the septum from both its left and right endocardial surfaces. Early contraction of the septum tends to make it more rigid and allows it to serve as an anchor point for the contraction of the remaining ventricular myocardium. Also, early contraction of the papillary muscles prevents eversion of the AV valves during ventricular systole.

The endocardial surfaces of both ventricles are activated rapidly, but the wave of excitation spreads from endocardium to epicardium at a slower velocity (about 0.3 to 0.4 m/sec). Because the right ventricular wall is appreciably thinner than the left, the epicardial surface of the right ventricle is activated earlier than that of the left ventricle. Also, apical and central epicardial regions of both ventricles are activated somewhat earlier than their respective basal regions. The last portions of the ventricles to be excited are the posterior basal epicardial regions and a small zone in the basal portion of the interventricular septum.

■ *Reentry*

Under certain conditions, a cardiac impulse may reexcite some myocardial region through which it had passed previously. This phenomenon, known as **reentry,** is responsible for many clinical **arrhythmias** (disturbances of cardiac rhythm). The reentry may be **ordered** or **random.** In the ordered variety the impulse traverses a fixed anatomic path, whereas in the random type the path continues to change.

The conditions necessary for reentry are illustrated in Fig. 22-30. In each of the four panels a single bundle *(S)* of cardiac fibers splits into a left *(L)* and right *(R)* branch. A connecting bundle *(C)* runs between the two branches. Normally the impulse moving down bundle *S* is conducted along the *L* and *R* branches (panel *A*). As the impulse reaches connecting link *C*, it enters from both sides and becomes extinguished at the point of collision. The impulse from the left side cannot proceed farther because the tissue beyond is absolutely refractory; it has just been depolarized from the other direction. The impulse also cannot pass through bundle *C* from the right, for the same reason.

Panel *B* shows that the impulse cannot complete the circuit if antegrade block exists in the *L* and *R* branches of the fiber bundle. Furthermore, if bidirectional block exists at any point in the loop (e.g., branch *R* in panel *C*), the impulse also cannot reenter.

A necessary condition for reentry is that at some point in the loop the impulse can pass in one direction but not in the other . This phenomenon is called **unidirectional block.** As shown in panel *D*, the impulse may travel down branch *L* normally and become blocked in the antegrade direction in branch *R*. The impulse that was conducted down branch *L* and through the connecting branch *C* may be able to penetrate the depressed region in branch *R* from the retrograde direction, even though the antegrade impulse had been blocked previously at this same site. Why is the antegrade impulse blocked but not the retrograde impulse? The reason is that the antegrade impulse arrives at the depressed region in branch *R* earlier than the retrograde impulse, because the retrograde impulse traverses a longer path. Therefore, the antegrade

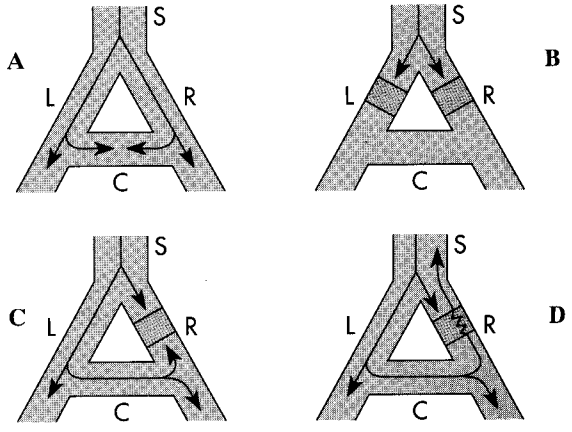

■ **Fig. 22-30** The role of unidirectional block in reentry. In **A,** an excitation wave traveling down a single bundle *(S)* of fibers continues down the left *(L)* and right *(R)* branches. The depolarization wave enters the connecting branch *(C)* from both ends and is extinguished at the zone of collision. In **B,** the wave is blocked in the *L* and *R* branches. In **C,** bidirectional block exists in branch *R*. In **D,** unidirectional block exists in branch *R*. The antegrade impulse is blocked, but the retrograde impulse is conducted through and reenters bundle *S*.

impulse may be blocked simply because it arrives at the depressed region during its effective refractory period. If the retrograde impulse is delayed sufficiently, the refractory period may have ended and the impulse can be conducted back into bundle *S*.

Although unidirectional block is a necessary condition for reentry, it alone cannot cause reentry. *For reentry to occur, the effective refractory period of the reentered region must be shorter than the propagation time around the loop.* In panel *D*, if the tissue just beyond the depressed zone in branch *R* is still refractory from the antegrade depolarization, the retrograde impulse will not be conducted into branch *S*. Therefore the conditions that promote reentry are those that prolong conduction time or shorten effective refractory period.

The functional components of the reentry loops responsible for specific arrhythmias in intact hearts are diverse. Some loops are large and involve entire specialized conduction bundles, whereas others are microscopic. The loop may include myocardial fibers, specialized conducting fibers, nodal cells, and junctional tissues in almost any conceivable arrangement. Also, cardiac cells in the loop may be normal or deranged.

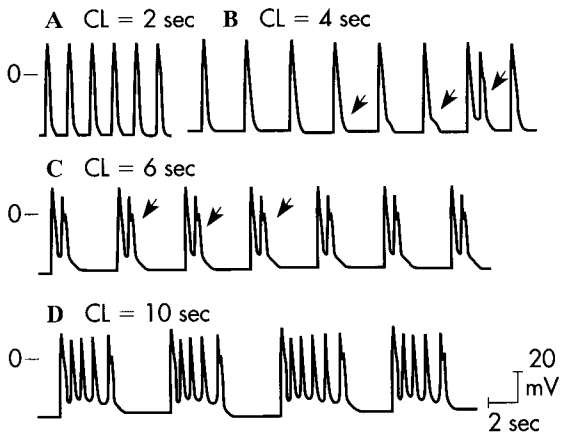

■ **Fig. 22-31** Effect of pacing at different cycle lengths *(CL)* on cesium-induced early afterdepolarizations (EADs) in a canine Purkinje fiber. **A,** EADs not evident. **B,** EADs first appear *(arrows)*. Third EAD reaches threshold and triggers an action potential *(third arrow)*. **C,** EADs that appear after each driven depolarization trigger an action potential. **D,** Triggered action potentials occur in salvos. (Modified from Damiano BP, Rosen M: *Circulation* 69:1013, 1984, with permission of the American Heart Association.)

■ *Triggered Activity*

Triggered activity is so named because it is always coupled to a preceding action potential. Because reentrant activity is also coupled to a preceding action potential, the arrhythmias induced by triggered activity are usually difficult to distinguish from those induced by reentry. Triggered activity is caused by **afterdepolarizations.** Two types of afterdepolarizations are recognized: **early (EAD)** and **delayed (DAD).** EADs appear at the end of the plateau (phase 2) or about midway through repolarization (phase 3), whereas DADs occur near the very end of repolarization or just after full repolarization (phase 4).

Early afterdepolarizations. EADs tend to appear near the end of the action potential plateau or during repolarization, but before the cell has fully repolarized. They are more likely to occur when the prevailing heart rate is slow; a rapid heart rate suppresses EADs. In the experiment shown in Fig. 22-31, EADs are induced by cesium in an isolated Purkinje fiber preparation. No afterdepolarizations are evident when the preparation is driven at a cycle length of 2 seconds. When the cycle length is increased to 4 seconds, however, EADs appear. Most of the EADs are subthreshold *(first two arrows)*, but one of the EADs reaches threshold and triggers an action potential. When the cycle length is increased to 6 seconds, each driven action potential generates an EAD that triggers a second action potential. Furthermore, when the cycle length is increased to 10 seconds, each driven action potential triggers a salvo of four or five additional action potentials.

EADs are more likely to occur in cardiac cells with prolonged action potentials than in cells with shorter action potentials. For example, EADs can be induced more readily in myocytes from the midmyocardial region of the ventricular walls than in myocytes from the endocardial or epicardial regions, owing to the disparity in these cells' action potential durations (Fig. 22-9). Furthermore, EADs may be produced experimentally by interventions that prolong the action potential. As we have seen, in the experiment shown in Fig. 22-31, EADs are more prevalent as the basic cycle length is increased. Such increases in basic cycle length do, of course, prolong the action potential (Fig. 22-17), and this prolongation undoubtedly contributes to the generation of the EADs. Certain antiarrhythmic drugs, such as **quinidine,** act to prolong the action potential. Consequently, these drugs increase the likelihood that EADs may occur. Hence, *antiarrhythmic drugs are also frequently proarrhythmic.*

The direct correlation between a cell's action potential duration and its susceptibility to EADs is probably related to the time required for the Ca^{++} channels in the cell membranes to recover from inactivation. When action potentials are sufficiently prolonged, those Ca^{++} channels that were activated at the beginning of the plateau have sufficient time to recover from inactivation and thus may be reactivated before the cell fully repolarizes. This secondary activation could then trigger an early afterdepolarization.

Delayed afterdepolarizations. In contrast to EADs, DADs are more likely to occur when the heart rate is high. The most important characteristics of DADs are shown in Fig. 22-32. In the experiment depicted in this

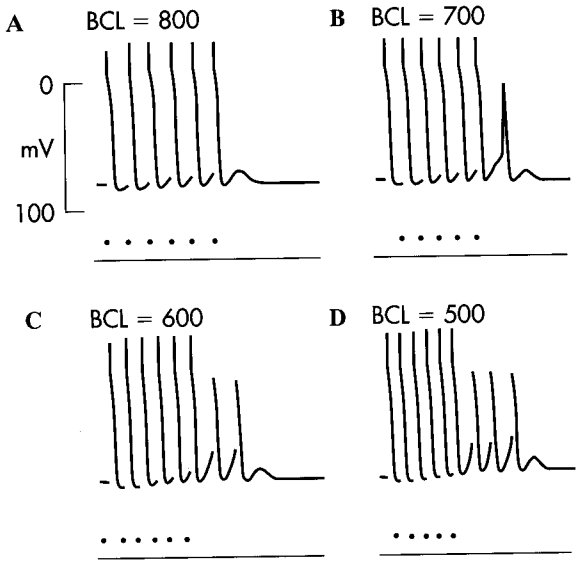

■ **Fig. 22-32** Transmembrane action potentials recorded from isolated canine Purkinje fibers. Acetylstrophanthidin, a digitalis-like agent, was added to the bath, and sequences of six driven beats (denoted by the dots) were produced at basic cycle lengths *(BCL)* of 800, 700, 600, and 500 msec. Note that delayed afterpotentials occurred after the driven beats, and that these afterpotentials reached threshold after the last driven beat in panels **B** to **D.** (From Ferrier GR, Saunders JH, Mendez C: *Circ Res* 32:600, 1973, with permission of the American Heart Association.)

figure, transmembrane potentials are recorded from Purkinje fibers exposed to a high concentration of acetylstrophanthidin, a digitalis-like substance. In the absence of any driving stimuli, these fibers are quiescent.

In each panel of Fig. 22-32, a sequence of six driven depolarizations is induced at a specific basic cycle length. When the cycle length is 800 msec (*A*), the last driven depolarization is followed by a brief, partial depolarization (DAD) that does not reach threshold. Once that afterdepolarization subsides, the transmembrane potential remains constant until another driving stimulus is given. The upstroke of a DAD can be detected after each of the first five driven depolarizations.

When the basic cycle length is reduced to 700 msec (*B*), the DAD that followed the last driven beat does reach threshold, and a nondriven depolarization (or extrasystole) ensues. This extrasystole is itself followed by an afterpotential that is subthreshold. Reducing the basic cycle length to 600 msec (*C*) also evokes an extrasystole after the last driven depolarization. The afterpotential that follows the extrasystole does reach threshold, however, and a second extrasystole occurs. When the six driven depolarizations are separated by intervals of 500 msec (*D*), a sequence of three extrasystoles follows. Slightly shorter basic cycle lengths or slightly greater concentrations of acetylstrophanthidin evoke a long sequence of nondriven beats; such a sequence resembles a paroxysmal tachycardia (Fig. 22-40).

DADs are associated with elevated intracellular Ca^{++} concentrations. The amplitudes of the DADs are increased by interventions that raise intracellular Ca^{++} concentrations. Such interventions include increasing the extracellular Ca^{++} concentration and administering toxic amounts of digitalis glycosides. The elevated levels of intracellular Ca^{++} provoke the oscillatory release of Ca^{++} from the sarcoplasmic reticulum. Hence, in myocardial cells, DADs are accompanied by small, rhythmic changes in developed force. The high intracellular Ca^{++} concentrations also activate certain membrane channels that permit the passage of Na^+ and K^+. The net flux of these cations constitutes a **transient inward current,** i_{ti}, that is at least partly responsible for the afterdepolarization of the cell membrane. The elevated intracellular Ca^{++} concentration may also activate Na^+, Ca^{++} exchange (see Chapter 1). This electrogenic exchanger, which pumps 3 Na^+ into the cell for each Ca^{++} it ejects, also creates a net inward current of cations that contributes to the DAD.

■ *Electrocardiography*

The ECG enables the physician to infer the course of the cardiac impulse by recording the variations in electrical potential at various loci on the surface of the body. By analyzing the details of these fluctuations of electrical potential, the physician gains valuable insight into (1) the anatomic orientation of the heart; (2) the relative sizes of its chambers; (3) various disturbances of rhythm and conduction; (4) the extent, location, and progress of ischemic damage to the myocardium; (5) the effects of altered electrolyte concentrations; and (6) the influence of certain drugs (notably digitalis, antiarrhythmic agents, and Ca^{++} channel antagonists). Because electrocardiography is an extensive and complex discipline, only elementary principles are considered in this section.

■ *Scalar Electrocardiography*

In electrocardiography a **lead** is the electrical connection from the patient's skin to the recording device (electrocardiograph). The leads are connected to a galvanometer (a device that measures the strength of an electrical current) within the electrocardiograph. The systems of leads used to record routine ECGs are oriented in certain planes of the body. The diverse electromotive forces that exist in the heart at any moment can be represented by a three-dimensional **vector** (a quantity with magnitude and direction). A system of recording leads oriented in a given plane detects only the projection of the three-dimensional vector on that plane. The potential difference between two recording electrodes represents the projection of the vector on the line between the two leads. Components of vectors projected on such lines are not

vectors but **scalar quantities** (having magnitude, but not direction). Hence, a recording of changes of the differences of potential between two points on the surface of the skin over time is called a scalar ECG.

The scalar ECG detects changes over time of the electrical potential between some point on the surface of the skin and an indifferent electrode, or between pairs of points on the skin surface. The cardiac impulse progresses through the heart in a complex, three-dimensional pattern. Hence, the precise configuration of the ECG varies from individual to individual, and in any given individual the pattern varies with the anatomic location of the leads. The graphic display of the electrical impulse recorded by an ECG is called a **tracing.**

In general, a tracing consists of P, QRS, and T waves (Fig. 22-33). The PR interval (or more precisely, the PQ interval) is a measure of the time from the onset of atrial activation to the onset of ventricular activation; it normally ranges from 0.12 to 0.20 second. A considerable fraction of this time involves passage of the impulse through the AV conduction system. *Pathological prolongations of the PR interval are associated with disturbances of AV conduction, which may be produced by inflammatory, circulatory, pharmacologic, or nervous mechanisms.*

The configuration and amplitude of the QRS complex vary considerably among individuals. The duration is usually between 0.06 and 0.10 second. An abnormally prolonged QRS complex may indicate a block in the normal conduction pathways through the ventricles (such as a block of the left or right bundle branch). During the ST interval, the entire ventricular myocardium is depolarized. Therefore, the ST segment normally lies on the **isoelectric line.** *Any appreciable deviation of the ST segment from the isoelectric line may indicate ischemic damage of the myocardium.* The QT interval is sometimes referred to as the period of "electrical systole" of the ventricles; the QT interval is closely correlated with the mean action potential duration of the ventricular myocytes. The QT interval duration is about 0.4 second, but it varies inversely with heart rate, mainly because the myocardial cell action potential duration varies inversely with heart rate (Fig. 22-17).

In most leads, the T wave is deflected in the same direction from the isoelectric line as is the major component of the QRS complex, although biphasic or oppositely directed T waves are perfectly normal in certain leads. When the T wave and QRS complex deviate in the same direction from the isoelectric line, it indicates that the repolarization process proceeds in a direction counter to the depolarization process. *T waves that are abnormal either in direction or in amplitude may indicate myocardial damage, electrolyte disturbances, or cardiac hypertrophy.*

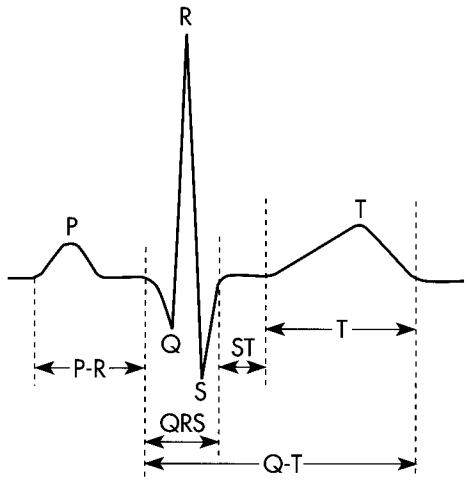

■ **Fig. 22-33** The important deflections and intervals of a typical scalar electrocardiogram.

■ *Standard Limb Leads*

The original ECG lead system was devised by Einthoven. In his lead system, the vector sum of all cardiac electrical activity at any moment is called the **resultant cardiac vector.** This directional electrical force is considered to lie in the center of an equilateral triangle whose apices are located in the left and right shoulders and the pubic region (Fig. 22-34). This triangle, called Einthoven's triangle, is oriented in the frontal plane of the body. Hence, only the projection of the resultant cardiac vector on the frontal plane is detected by this system of leads. For convenience, the electrodes are connected to the right and left forearms rather than to the corresponding shoulders, because the arms represent simple extensions of the leads from the shoulders. Similarly, the leg represents an extension of the lead system from the pubis, and thus the third electrode is usually connected to an ankle (usually the left one).

Certain conventions dictate the manner in which these standard limb leads are connected to the galvanometer. Lead I records the potential difference between the left arm *(LA)* and the right arm *(RA)*. The galvanometer connections are such that when the potential at *LA* (V_{LA}) exceeds the potential at *RA* (V_{RA}), the galvanometer stylus is deflected upward from the isoelectric line. In Figs. 22-34 and 22-35, this arrangement of the galvanometer connections for lead I is designated by a (+) at *LA* and by a (−) at *RA*. Lead II records the potential difference between *RA* and *LL* (left leg), and the stylus is deflected upward when V_{LL} exceeds V_{RA}. Finally, lead III registers the potential difference between *LA* and *LL*, and the stylus is deflected upward when V_{LL} exceeds V_{LA}. These galvanometer connections were arbitrarily chosen so that the QRS complexes are upright in all three standard limb leads in most normal individuals.

Let the frontal projection of the resultant cardiac vector at some moment be represented by an arrow (tail negative, head positive), as in Fig. 22-34. The potential dif-

ference, $V_{LA} - V_{RA}$, recorded in lead I is represented by the component of the vector projected along the horizontal line between *LA* and *RA*, also shown in Fig. 22-34. If the vector makes an angle, Θ, of 60 degrees with the horizontal line (as in Fig. 22-35, *A*), the magnitude of the potential recorded by lead I equals the vector magnitude times cosine 60 degrees. The deflection recorded in lead I is upward because the positive arrowhead lies closer to *LA* than to *RA*. The deflection in lead II is also upright because the arrowhead lies closer to *LL* than to *RA*. The magnitude of the lead II deflection is greater than that in lead I because in this example the direction of the vector parallels that of lead II; therefore, the magnitude of the projection on lead II exceeds that on lead I. Similarly, in lead III, the deflection is upright and its magnitude equals that in lead I.

If the vector in Fig. 22-35, *A* is the result of electrical events that occur during the peak of the QRS complex, the orientation of this vector is said to represent the **mean electrical axis** of the heart in the frontal plane. The positive direction of this axis is taken in the clockwise direction from the horizontal plane (contrary to the usual mathematical convention). In normal individuals, the average mean electrical axis is approximately + 60 degrees (as in Fig. 22-35, *A*). Therefore, the QRS complexes are usually upright in all three leads and largest in lead II.

Changes in the mean electrical axis may occur if the anatomic position of the heart is altered or in certain cardiovascular disturbances that alter the relative mass of the right and left ventricles. For example, the axis tends to shift toward the left (more horizontal) in short, stocky individuals and toward the right (more vertical) in tall, thin persons. Also, in left or right **ventricular hypertrophy** (increased myocardial mass of either ventricle), the axis shifts toward the hypertrophied side.

If the mean electrical axis shifts substantially to the right (as in Fig. 22-35, *B*, where Θ = 120 degrees), the projections of the QRS complexes on the standard leads change considerably. In this case, the largest upright deflection is in lead III, and the deflection in lead I is inverted because the arrowhead is closer to *RA* than to *LA*. When the axis shifts to the left (Fig. 22-35, *C*, where Θ = 0 degrees), the largest upright deflection is in lead I, and the QRS complex in lead III is inverted.

In addition to limb leads I, II, and III, other limb leads that are also oriented in the frontal plane are routinely recorded in patients. The axes of such **unipolar limb leads** form angles of + 90, −30, and −150 degrees with

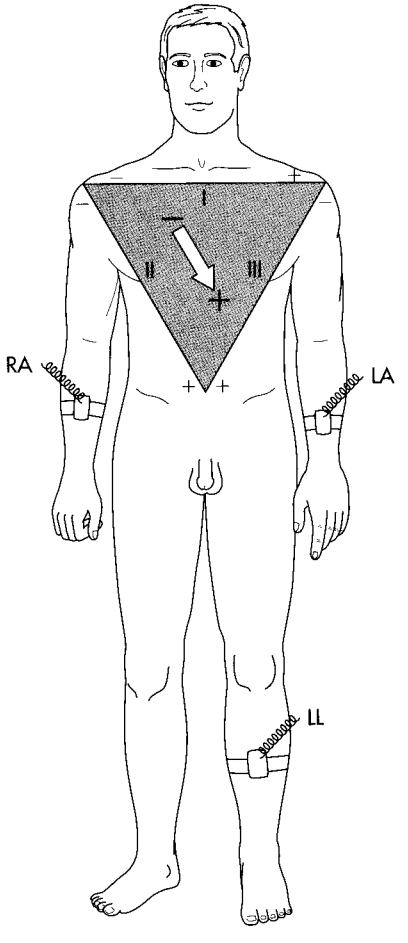

■ **Fig. 22-34** Einthoven triangle, illustrating the galvanometer connections for standard limb leads I, II, and III.

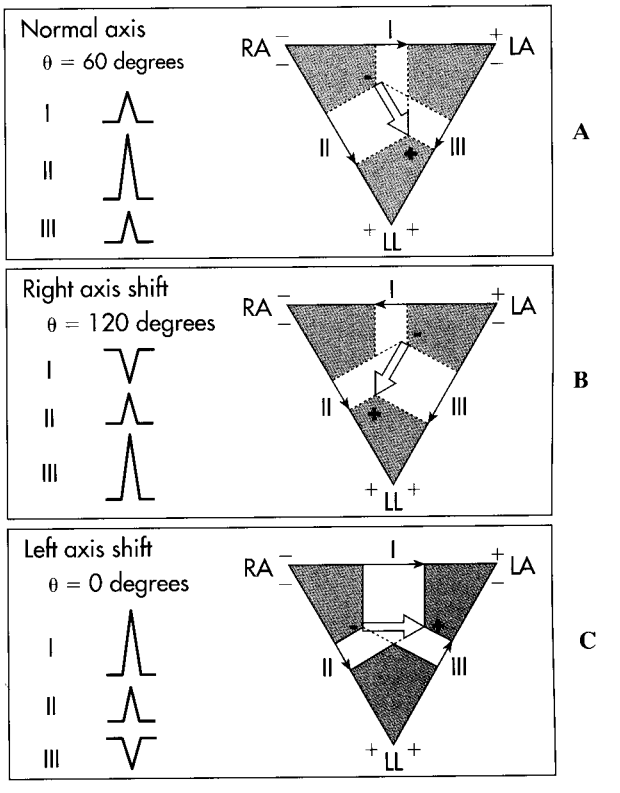

■ **Fig. 22-35** Magnitude and direction of the QRS complexes in limb leads I, II, and III, when the mean electrical axis (Θ) is 60 degrees **(A)**, 120 degrees **(B)**, and 0 degrees **(C)**.

the horizontal axis. Furthermore, the **precordial leads** are also recorded to determine the projections of the cardiac vector on the sagittal and transverse planes of the body. These precordial leads are recorded from six selected points on the anterior and lateral surfaces of the chest in the vicinity of the heart. The unipolar and precordial lead systems are described in all textbooks on electrocardiography and are not considered further here.

■ *Arrhythmias*

Cardiac arrhythmias reflect disturbances of either **impulse initiation** or **impulse propagation.** Disturbances of impulse initiation include those that arise from the SA node and those that originate from various ectopic foci. The principal disturbances of impulse propagation are conduction blocks and reentrant rhythms.

■ *Altered Sinoatrial Rhythms*

Earlier in this chapter, mechanisms that vary the firing frequency of cardiac pacemaker cells were described (Fig. 22-20). Changes in the SA nodal firing rate are usually produced by the cardiac autonomic nerves. Examples of ECGs of **sinus tachycardia** and **sinus bradycardia** are shown in Fig. 22-36. The P, QRS, and T deflections are all normal, but the cardiac cycle duration (the PP interval) is altered. Characteristically, in response to sinus bradycardia or tachycardia development, cardiac frequency changes gradually, and several beats are required to attain its new steady-state value. ECG evidence of respiratory cardiac arrhythmia is common and manifests as a rhythmic variation in the PP interval at the respiratory frequency (Fig. 24-10).

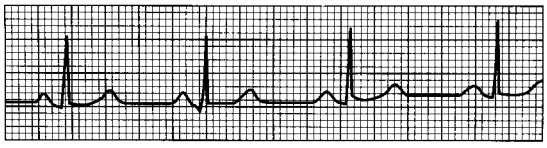

A, Normal sinus rhythm.

B, Sinus tachycardia.

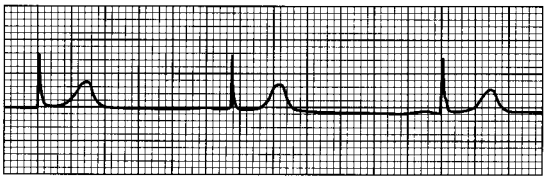

C, Sinus bradycardia.

■ **Fig. 22-36** **A** to **C,** Sinoatrial rhythms.

■ *Atrioventricular Conduction Blocks*

Various physiological, pharmacologic, and pathological processes can impede impulse transmission through the AV conduction tissue. The site of block can be localized more precisely by recording the **His bundle electrogram** (Fig. 22-37). To obtain such tracings, an electrode catheter is introduced into a peripheral vein and threaded centrally until the electrode lies in the AV junctional region. When the electrode is properly positioned, a distinct deflection (*H* in Fig. 22-37) is registered as the cardiac impulse passes through the bundle of His. The time intervals required for propagation from the atrium to the bundle of His (A-H interval) and from the bundle of His to the ventricles (H-V interval) may be measured accurately. Abnormal prolongation of the former or latter interval indicates block above or below the bundle of His, respectively.

Three degrees of AV block can be distinguished, as shown in Fig. 22-38. **First-degree AV block** is characterized by a prolonged P-R interval. In Fig. 22-38, *A*, the PR interval is 0.28 second; an interval greater than 0.20 second is abnormal. In most cases of first-degree block, the A-H interval is prolonged and the H-V interval is normal. Hence, the delay in a first-degree AV block is located above the His bundle (i.e., in the AV node).

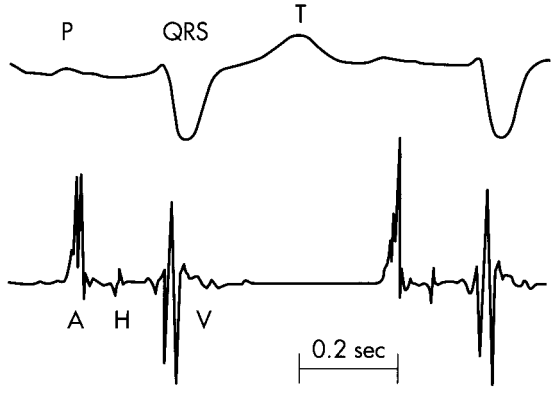

■ **Fig. 22-37** His bundle electrogram (*lower tracing,* retouched) and lead II of the scalar electrocardiogram (*upper tracing*). The deflection, *H,* which represents the impulse conduction over the bundle of His, is clearly visible between the atrial *(A)* and the ventricular *(V)* deflections. The conduction time from the atria to the bundle of His is denoted by the A-H interval; that from the bundle of His to the ventricles, by the H-V interval. (Courtesy of Dr. J. Edelstein.)

In **second-degree AV block,** all QRS complexes are preceded by P waves, but not all P waves are followed by QRS complexes. The ratio of P waves to QRS complexes is usually the ratio of two small integers (such as 2:1, 3:1, or 3:2). Fig. 22-38, *B* illustrates a typical 2:1 block. The site of block may be located above or below the His bundle. A block below the bundle is usually more serious than one above the bundle, because the former is more likely to evolve into a third-degree block. An artificial pacemaker is frequently implanted when the block is below the bundle.

Third-degree AV block is often referred to as **complete heart block** because the impulse is completely unable to traverse the AV conduction pathway from atria to ventricles. The most common sites of complete block are distal to the bundle of His. In complete heart block, the atrial and ventricular rhythms are entirely independent, as shown in Fig. 22-38, *C*. Because of the slow ventricular rhythm (32 beats/min in this example), the distribution of blood flow to the body is often inadequate, especially during muscular activity. Third-degree block is often associated with **syncope** (pronounced lightheadedness), which is caused principally by insufficient cerebral blood flow. Third-degree block is one of the most common conditions that require artificial pacemakers.

■ *Premature Depolarizations*

Premature depolarizations occur occasionally in most normal individuals, but they arise more commonly under certain abnormal conditions. They may originate in the atria, AV junction, or ventricles. One type of premature depolarization follows a normally conducted depolarization after a constant time interval (the **coupling interval**). If the normal depolarization is suppressed in some way (e.g., by vagal stimulation), the premature depolarization is also abolished. Such premature depolarizations are called **coupled extrasystoles,** or simply **extrasystoles,** and they probably reflect a reentry phenomenon (Fig. 22-30). A second type of premature depolarization occurs as the result of enhanced automaticity in some ectopic focus. This ectopic center may fire regularly, and a zone of tissue that conducts unidirectionally may protect this center from being depolarized by the normal cardiac impulse. If this premature depolarization occurs at a regular interval or at an integer multiple of that interval, the disturbance is called **parasystole.**

A **premature atrial depolarization** is shown in Fig. 22-39, *A*. In the tracing, the normal interval between beats is 0.89 second (heart rate, 68 beats/min). The premature atrial depolarization (second P wave in the figure) follows the preceding P wave by only 0.56 second. The

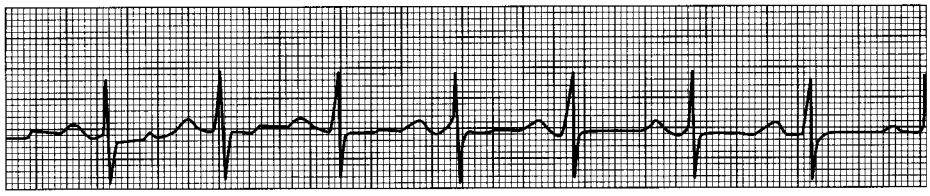

A, First-degree AV block.

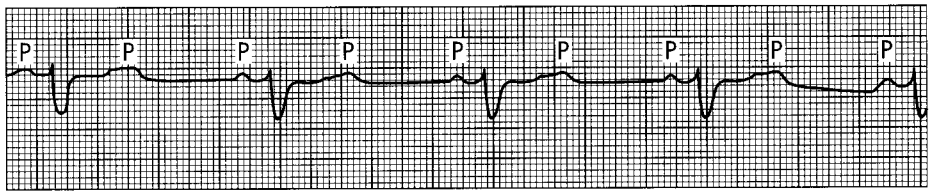

B, Second-degree AV block (2:1).

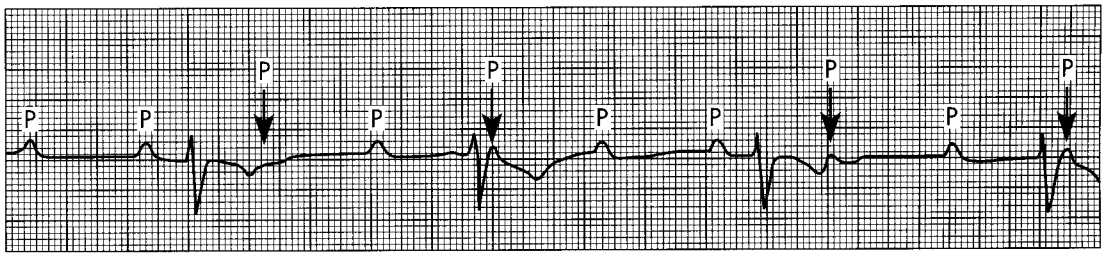

C, Third-degree AV block.

■ **Fig. 22-38** AV blocks. **A,** First-degree block; PR interval is 0.28 second. **B,** Second-degree block (2:1). **C,** Third-degree block; note the dissociation between the P waves and the QRS complexes.

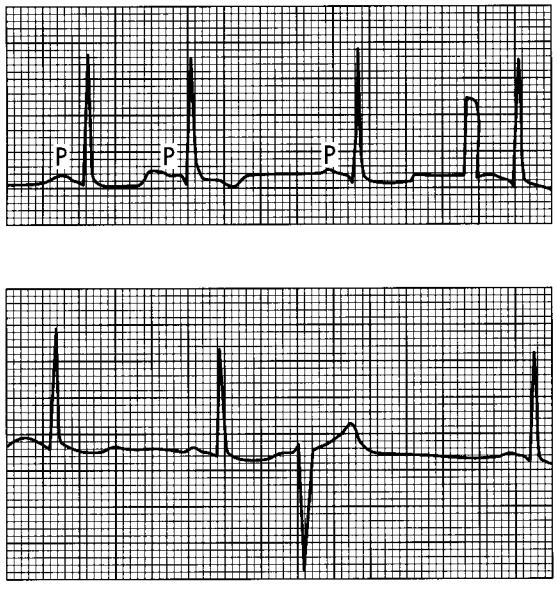

■ **Fig. 22-39** A premature atrial depolarization **(A)** and a premature ventricular depolarization **(B).** The premature atrial depolarization (the second beat in the top tracing) is characterized by an inverted P wave and normal QRS and T waves. The interval after the premature depolarization is not much longer than the usual interval between beats. The brief rectangular deflection just before the last depolarization is a standardization signal. The premature ventricular depolarization is characterized by bizarre QRS and T waves and is followed by a compensatory pause.

configuration of the premature P wave differs from the configuration of the other, normal P waves because the course of atrial excitation, which originates at some ectopic focus in the atrium, differs from the normal spread of excitation, which originates at the SA node. The configuration of the QRS complex of the premature depolarization is usually normal because the ventricular excitation spreads over the usual pathways.

A **premature ventricular depolarization** appears in Fig. 22-39, *B*. Because the premature excitation originates at some ectopic focus in the ventricles, the impulse propagation is abnormal and the configurations of the QRS and T waves are entirely different from the normal deflections. The premature QRS complex follows the preceding normal QRS complex by only 0.47 second. The interval after the premature excitation is 1.28 seconds, which is considerably longer than the normal interval between beats (0.89 second). The interval (1.75 seconds) from the QRS complex just before the premature excitation to the QRS complex just after it is virtually equal to the duration of two normal cardiac cycles (0.89 + 0.89 = 1.78 seconds).

The prolonged interval that usually follows a premature ventricular depolarization is called a **compensatory pause.** This pause occurs because the ectopic ventricular impulse does not disturb the natural rhythm of the SA node, either because the ectopic ventricular impulse is not conducted retrograde through the AV conduction system or because the SA node had already fired at its natural interval before the ectopic impulse could have reached it and depolarized it prematurely. Likewise, the SA nodal impulse generated just before or after the ventricular extrasystole usually does not affect the ventricle, because the AV junction and perhaps also the ventricles are still refractory from the premature excitation. In Fig. 22-39, *B*, the P wave associated with the extrasystole occurs synchronously with the T wave of the premature ventricular depolarization, and therefore it cannot easily be identified in the tracing.

■ *Ectopic Tachycardias*

In contrast to the gradual rate changes that characterize sinus tachycardia, tachycardias that originate from an ectopic focus typically begin and end abruptly. Hence, such ectopic tachycardias are usually called **paroxysmal tachycardias.** Episodes of paroxysmal tachycardia may persist for only a few beats or for many hours or days, and episodes often recur. Paroxysmal tachycardias may result from (1) the rapid firing of an ectopic pacemaker, (2) triggered activity secondary to afterpotentials that reach threshold, or (3) an impulse that circles a reentry loop repetitively.

Paroxysmal tachycardias that originate in the atria or in the AV junctional tissues (Fig. 22-40, *A*) are usually indistinguishable, and therefore both are included in the term **paroxysmal supraventricular tachycardia.** In this tachycardia, the impulse often circles a reentry loop that includes atrial and AV junctional tissue. The QRS complexes are often normal, because ventricular activation proceeds over the usual pathways.

As its name implies, **paroxysmal ventricular tachycardia** originates from an ectopic focus in the ventricles. The ECG is characterized by repeated, bizarre QRS complexes that reflect the abnormal intraventricular impulse conduction (Fig. 22-40, *B*). Paroxysmal ventricular tachycardia is much more ominous than supraventricular tachycardia, because the former is frequently a precursor of ventricular fibrillation, a lethal arrhythmia described in the next section.

■ *Fibrillation*

Under certain conditions, cardiac muscle undergoes an irregular type of contraction that is entirely ineffectual in propelling blood. Such an arrhythmia is termed **fibrillation,** and the disturbance may involve either the atria or the ventricles. Fibrillation probably represents a reentry phenomenon, in which the reentry loop fragments into multiple, irregular circuits.

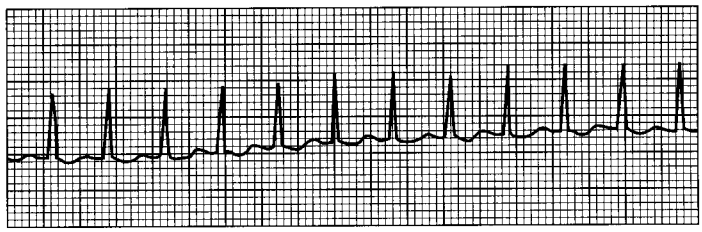

A, Supraventricular tachycardia.

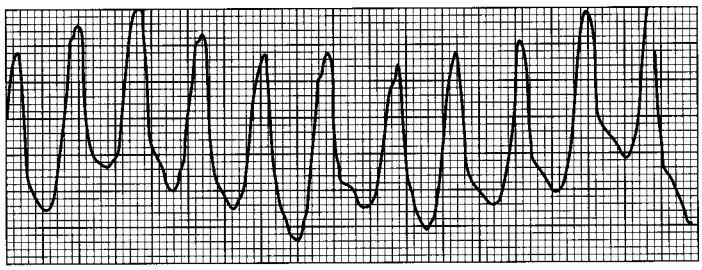

B, Ventricular tachycardia.

■ **Fig. 22-40** **A** and **B,** Paroxysmal tachycardias.

The ECG changes in **atrial fibrillation** are shown in Fig. 22-41, *A*. This arrhythmia occurs in various types of chronic heart disease. The atria do not contract and relax sequentially during each cardiac cycle, and thus they do not contribute to ventricular filling. Instead, the atria undergo a continuous, uncoordinated, rippling motion. P waves do not appear in the ECG; they are replaced by continuous irregular fluctuations of potential, called **f waves.** The AV node is activated at intervals that may vary considerably from cycle to cycle. Hence, no constant interval occurs between successive QRS complexes or between successive ventricular contractions. Because the strength of ventricular contraction depends on the interval between beats (as explained on p 390), the volume and rhythm of the pulse are irregular. In many patients, the atrial reentry loop and the pattern of AV conduction are more regular than they are in atrial fibrillation. The rhythm is then referred to as **atrial flutter.**

Atrial fibrillation and flutter are not life threatening; some people with these disturbances can even perform full activity. **Ventricular fibrillation,** on the other hand, leads to loss of consciousness within a few seconds. The irregular, continuous, uncoordinated twitchings of the ventricular muscle fibers pump no blood. Death ensues unless immediate effective resuscitation is achieved or unless the rhythm spontaneously reverts to normal, which rarely occurs. Ventricular fibrillation may supervene when the entire ventricle, or some portion of it, is deprived of its normal blood supply. It may also occur as a result of electrocution or in response to certain drugs and anesthetics. In the ECG (Fig. 22-41, *B*), irregular fluctuations of potential are manifested.

Ventricular fibrillation is often initiated when a premature impulse arrives during the **vulnerable period,** which coincides with the downslope of the T wave of the ECG. During this period, the excitability of the cardiac cells varies spatially. Some fibers are still in their effective refractory periods; others have almost fully recovered their excitability; and still others are able to conduct impulses but only at very slow conduction velocities. Consequently, the action potentials are propagated over the chambers in many irregular wavelets that travel along circuitous paths and at various conduction velocities. As a region of cardiac cells becomes excitable again, it is ultimately reentered by one of the wave fronts traveling around the chamber. Hence, the process is self-sustaining.

Atrial fibrillation may be changed to a normal sinus rhythm by drugs that prolong the refractory period. As the cardiac impulse completes the reentry loop, it may then encounter the myocardial fibers that are no longer excitable. However, dramatic therapy is required in ventricular fibrillation. Conversion to a normal sinus rhythm is accomplished by means of a strong electrical current that places the entire myocardium briefly in a refractory state. Techniques have been developed to safely administer the current through the intact chest wall. In successful cases, the SA node again takes over the normal pacemaker function for the entire heart. When atrial defibrillation does not respond adequately to drugs, electrical defibrillation may also be used to correct this condition.

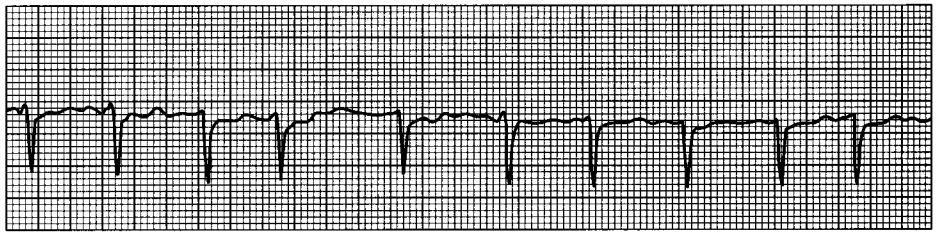

A, Atrial fibrillation.

B, Ventricular fibrillation.

■ **Fig. 22-41** Atrial and ventricular fibrillation.

■ *Summary*

1. The transmembrane action potentials that can be recorded from cardiac myocytes contain the following five phases:
   - Phase 0: The action potential upstroke is produced when a suprathreshold stimulus rapidly depolarizes the membrane by activating the fast Na^+ channels.
   - Phase 1: The notch is an early partial repolarization that is achieved by the efflux of K^+ through transmembrane channels that conduct the transient outward current, i_{to}.
   - Phase 2: The plateau represents a balance between the influx of Ca^{++} through transmembrane Ca^{++} channels and the efflux of K^+ through several types of K^+ channels.
   - Phase 3: Final repolarization is initiated when the efflux of K^+ exceeds the influx of Ca^{++}. The resultant partial repolarization rapidly increases the K^+ conductance and rapidly restores full repolarization.
   - Phase 4: The resting potential of the fully repolarized cell is determined mainly by conductance of the cell membrane to K^+ through i_{K1} channels.

2. Fast-response action potentials are recorded from atrial and ventricular myocardial fibers and from ventricular specialized conducting (Purkinje) fibers. The action potential is characterized by a large amplitude, a steep upstroke, and a relatively long plateau.

3. The effective refractory period of fast-response fibers begins at the upstroke of the action potential and persists until midway through phase 3. The fiber is relatively refractory during the remainder of phase 3, and it regains full excitability when it is fully repolarized (phase 4).

4. Slow-response action potentials are recorded from normal SA and AV nodal cells and from abnormal myocardial cells that have been partially depolarized. The action potential is characterized by a less negative resting potential, a smaller amplitude, a less steep upstroke, and a shorter plateau than is the fast-response action potential. The upstroke is produced by the activation of Ca^{++} channels.

5. Slow-response fibers become absolutely refractory at the beginning of the upstroke, and partial excitability may not be regained until very late in phase 3 or until after the fiber is fully repolarized.

6. Automaticity is characteristic of certain cells in the SA and AV nodes and in the ventricular specialized conducting system. Slow depolarization of the membrane during phase 4 is the hallmark of automaticity.

7. Normally the SA node initiates the impulse that induces cardiac contraction. This impulse is propagated from the SA node to the atrial tissues and ultimately reaches the AV node. After a delay in the AV node, the cardiac impulse is propagated throughout the ventricles.

8. Ectopic foci in the atrium, AV node, or His-Purkinje system may initiate propagated cardiac impulses if the normal pacemaker cells in the SA node are suppressed or if the rhythmicity of the ectopic automatic cells is abnormally enhanced.

9. Under certain abnormal conditions, afterdepolarizations may appear early in phase 3 of a normally initiated beat, or the afterdepolarizations may be delayed until near the end of phase 3 or the beginning of phase 4. Such afterdepolarizations may themselves trigger propagated impulses. Early afterdepolarizations are more likely to occur when the basic cycle length of the initiating beats is very long and when the cardiac action potentials are abnormally prolonged. Delayed afterdepolarizations are more likely to occur when the basic cycle length of the initiating beats is short and when the cardiac cells are overloaded with Ca^{++}.

10. Simple conduction block is the retardation or failure of impulse propagation in a cardiac fiber.

11. A cardiac impulse may traverse a loop of cardiac fibers and reenter previously excited tissue when the impulse is conducted slowly around the loop, and when the impulse is blocked unidirectionally in some section of the loop.

12. The electrocardiogram (ECG), which is recorded from the surface of the body, traces the conduction of the cardiac impulse throughout the heart.

13. The ECG may be used to detect and analyze certain cardiac arrhythmias, such as altered sinoatrial rhythms, AV conduction blocks, premature depolarizations, ectopic tachycardias, and atrial and ventricular fibrillation.

■ *Self-Study Problems*

1. What major movements of ions account for each phase of the action potential of a typical fast-response myocardial cell?

2. Why is the cardiac action potential propagated more slowly in an AV node cell than in an atrial or ventricular myocyte?

3. By what pathways does a cardiac impulse that originates in the SA node arrive in the ventricular myocardium?

4. What electrophysiological conditions lead to reentry?

5. What electrocardiographic changes occur in first-, second-, and third-degree AV block?

■ *Bibliography*

Journal articles

Antzelevitch C, Sicouri S: Clinical relevance of cardiac arrhythmias generated by afterdepolarization: role of M cells in the generation of U waves, triggered activity and torsade de pointes, *J Am Coll Cardiol* 23:259, 1994.

Balke CW et al: Biophysics and physiology of cardiac calcium channels, *Circulation* 87:VII-49, 1993.

Beaumont J et al: A model study of changes in excitability of ventricular muscle cells: inhibition, facilitation, and hysteresis, *Am J Physiol* 268:H1181, 1995.

Billette J, Nattel S: Dynamic behavior of the atrioventricular node: a functional model of interaction between recovery, facilitation, and fatigue, *J Cardiovasc Electrophysiol* 5:90, 1994.

Delmar M: Role of potassium currents on cell excitability in cardiac ventricular myocytes, *J Cardiovasc Electrophysiol* 3:474, 1993.

Demir SS, Clark JW, Murphey CR, Giles WR: A mathematical model of a rabbit sinoatrial node cell, *Am J Physiol* 266:C832, 1994.

DiFrancesco D: Pacemaker mechanisms in cardiac tissue, *Annu Rev Physiol* 55:455, 1993.

Grant AO: Evolving concepts of cardiac sodium channel function, *J Cardiovasc Electrophysiol* 1:53, 1990.

Irisawa H, Brown HF, Giles W: Cardiac pacemaking in the sinoatrial node, *Physiol Rev* 73:197, 1993.

January CT, Shorofsky S: Early afterdepolarizations: newer insights into cellular mechanisms, *J Cardiovasc Electrophysiol* 1:161, 1990.

Levy MN: Role of calcium in arrhythmogenesis, *Circulation* 80:IV-23, 1989.

Liu D-W, Gintant GA, Antzelevitch C: Ionic bases for electrophysiological distinctions among epicardial, midmyocardial, and endocardial myocytes from the free wall of the canine left ventricle, *Circ Res* 72:671, 1993.

Meijler FL, Janse MJ: Morphology and electrophysiology of the mammalian atrioventricular node, *Physiol Rev* 68:608, 1988.

Nichols CG et al: Inward rectification and implications for cardiac excitability, *Circ Res* 78:1, 1996.

Reiter M: Calcium mobilization and cardiac inotropic mechanisms, *Pharmacol Rev* 40:189, 1988.

Rosen MR: Links between basic and clinical cardiac electrophysiology, *Circulation* 77:251, 1988.

Schuessler RB, Boineau JP, Bromberg BI: Origin of the sinus impulse, *J Cardiovasc Electrophysiol* 7:263, 1996.

Sicouri S, Antzelevitch C: Electrophysiologic characteristics of M cells in the canine left ventricular free wall, *J Cardiovasc Electrophysiol* 6:591, 1995.

Spach MS, Josephson ME: Initiating reentry: the role of nonuniform anisotrophy in small circuits, *J Cardiovasc Electrophysiol* 5:182, 1994.

Waldo AL, Wit AL: Mechanisms of cardiac arrhythmias, *Lancet* 341:1189, 1993.

Books and monographs

Armour JA, Ardell JL: *Neurocardiology,* New York, 1994, Oxford University Press.

Cranefield PF, Aronson RS: *Cardiac arrhythmias: the role of triggered activity and other mechanisms,* Mt. Kisco, NY, 1988, Futura Publishing.

Dangman KH, Miura DS: *Electrophysiology and pharmacology of the heart: a clinical guide,* New York, 1991, Marcel Dekker.

Fozzard HA et al: *Heart and cardiovascular system. Scientific foundations,* New York, 1991, Raven Press.

Hille B: *Ionic channels of excitable membranes,* ed 2, Sunderland, Mass, 1991, Sinauer Associates.

Langer GA, editor: *Calcium and the heart,* New York, 1990, Raven Press.

Levy MN, Schwartz PJ: *Vagal control of the heart: experimental basis and clinical implications,* Armonk, NY, 1994, Futura Publishing.

Mazgalev T, Dreifus LS, Michelson EL: *Electrophysiology of the sinoatrial and atrioventricular nodes,* New York, 1988, Alan R Liss.

Sperelakis N: *Physiology and pathophysiology of the heart,* ed 3, Boston, 1995, Kluwer Academic.

Spooner PM et al: *Ion channels in the cardiovascular system: function and dysfunction,* Armonk, NY, 1994, Futura Publishing.

Wit AL, Janse MJ: *Ventricular arrhythmias of ischemia and infarction: electrophysiological mechanisms,* Armonk, NY, 1993, Futura Publishing.

Zipes DP, Jalife J: *Cardiac electrophysiology: from cell to bedside,* ed 2, Philadelphia, 1995, WB Saunders.